# Characterization of sterile tassel silky earl: A Homeotic B-Class Gene Involved in Specification of Floral Organ Identity In Zea mays

Steven Keith Williams
*Brigham Young University - Provo*

Characterization of *sterile tassel silky ear1*: a Homeotic B-class

Gene Involved in Specification of Floral Organ

Identity in *Zea mays*

Steven K. Williams

A thesis submitted to the faculty of
Brigham Young University
in partial fulfillment of the requirements for the degree of

Master of Science

Clinton Whipple, Chair
Leigh Johnson
Joshua Udall

Department of Biology

Brigham Young University

December 2012

ABSTRACT

Characterization of *sterile tassel silky ear1*: a Homeotic B-class
Gene Involved in Specification of Floral Organ
Identity in *Zea mays*

Steven Williams
Department of Biology, BYU
Master of Science

Specification of floral organ identity in angiosperm flowers is accomplished by the coordinated activity of A-, B-, C-, and E-class MADS-box genes.  In the eudicots, B-class genes specify petal and stamen identity.  This eudicot B-class function depends on the simultaneous expression of genes from two paralogous B-class lineages (the *DEFICIENS/APETALA3* lineage and the *GLOBOSA/PISTILLATA* lineage).  Proteins produced by genes from these two lineages interact as obligate heterodimers and together regulate the transcription of various downstream targets.  These obligate heterodimers also positively regulate the transcription of the B-class genes themselves, thereby mediating a unique B-class autoregulatory feedback loop.

There is compelling evidence that B-class function at the phenotypic and molecular level is highly conserved among the eudicots.  The degree to which B-class homeotic function, obligate heterodimerization, and autoregulation are conserved in non-eudicot, however, remains a topic of debate.  Here we describe loss of function in *Sterile tassel silky ear1* (*Sts1*) a maize ortholog of *GLOBOSA/PISTILLATA* formerly known as *Zmm16*.  Mutation in *Sts1* results in homeotic transformation of lodicules and stamens into bract-like organs in male inflorescences. Female inflorescences are affected in a similar manner.  Stamens in these inflorescences are, however, transformed into carpels instead of into bract-like organs.  This mutant phenotype suggests that *Sts1* has a B-class homeotic function.  Using qRT-PCR we also demonstrate that *Sts1* participates in positive transcriptional regulation of all of the maize B-class genes.  These findings suggest a high degree of B-class functional conservation between the monocots and the eudicots.  Analysis of *tasselseed1/sts1* and *grassy tillers1/sts1* double mutants suggests that maize B-class genes also play a role in the sex determination process.

## ACKNOWLEDGEMENTS

TABLE OF CONTENTS

# LIST OF TABLES AND FIGURES

**INTRODUCTION**

**The ABCs of angiosperm floral development**

The angiosperms are a highly diverse group of vascular plants that are defined in part by the containment of their reproductive organs within specialized structures known as flowers. Since their origin between 167 and 275 million years ago (Bell et al., 2010; Magallon, 2010; Smith et al., 2010) the angiosperms have evolved an incredible variety of floral morphologies. Interspecific variation in flower shape, sexuality (i.e. bisexual or unisexual), organ number, patterning, and identity is common among the angiosperms.

Over the past thirty years significant progress has been made in elucidating the genetic and molecular mechanisms responsible for floral development in the angiosperms. Much of this progress has been achieved via studies of two model eudicots, *Antirrhinum majus* and *Arabidopsis thaliana*. Although the flowers of *Antirrhinum* and *Arabidopsis* differ in their shape and the number of floral organ that they contain, flowers from both species consist of four floral organ types organized within four concentric regions, or whorls, of the flower. Analysis of mutants affecting the identity of these floral organs gave rise to what is now known as the ABC model of floral development (Bowman et al., 1991; Coen and Meyerowitz, 1991). According to this model, floral organ identity is specified by the activity of three classes of homeotic genes. Each class of gene acts alone or in combination with the other classes of floral homeotic genes to specify organ identity in two adjacent whorls of the developing flower. A-class genes act in the two outermost whorls of the flower (whorls 1 and 2), while B-class genes act in whorls 2 and 3, and C-class genes act in the two innermost whorls (whorls 3 and 4). A-class genes acting alone in whorl 1 specify sepal identity, while combinatorial A- and B-class gene activity in whorl 2 specifies petal identity. Combined B- and C-class activity in whorl 3 establishes stamen identity,

and solitary C-class activity in whorl 4 specifies carpel identity. Respective restriction of A-class gene activity and C-class gene activity to the two outermost and the two innermost whorls is due to mutual antagonism between these gene classes. This model was later expanded to include an additional class of floral homeotic genes known as the E-class. E-class genes are expressed throughout the entire flower and are necessary for specification of floral organ identity in all four whorls (Honma and Goto, 2001; Pelaz et al., 2000).

Molecular characterization of the floral organ identity genes of *Antirrhinum* and *Arabidopsis* has revealed that, with the exception of one A-class gene, all of the A-, B-, C-, and E-class genes belong to the MIKC-type subfamily of MADS-box transcription factors (Bradley et al., 1993; Davies et al., 1999; Ditta et al., 2004; Goto and Meyerowitz, 1994; Huijser et al., 1992; Jack et al., 1992; Jofuku et al., 1994; Keck et al., 2003; Liljegren et al., 2000; Mandel et al., 1992; Okamuro et al., 1997; Pelaz et al., 2000; Sommer et al., 1990; Trobner et al., 1992; Yanofsky et al., 1990). MIKC-type MADS-box proteins all contain a conserved domain structure consisting of a MADS (M), intervening (I), keratin-like (K), and C terminal (C) domain. The MADS domain is primarily involved in DNA binding although it has been shown to also play a role in protein dimerization. The I and K domains are also involved in dimer formation and seem to play important roles in dimerization specificity. The function of the C terminal domain, however, is still relatively unclear although some evidence suggests that it is involved in the formation of higher-order protein complexes (Krizek and Meyerowitz, 1996b; Riechmann et al., 1996; see Immink et al., 2010 for review). A-, B-, C-, and E-class membership in the MIKC-type MADS-box gene family suggests that the homeotic role of these floral organ identity genes is accomplished via the binding of their protein products to DNA and the subsequent transcriptional regulation of downstream targets. *In planta* nuclear localization of A-

, B-, C-, and E-class proteins provides further support for their proposed functional role as transcriptional regulators (McGonigle et al., 1996; Urbanus et al., 2009).

**A-, B-, C-, and E-class protein-protein interactions**

Like most transcription factors A-, B-, C-, and E-class proteins only function in dimeric or multimeric form. *In planta* studies of MIKC-type MADS-box proteins show that dimerization is essential for proper entry of several of the A-, B-, C-, and E-class proteins into the plant cell nucleus (Immink et al., 2002; McGonigle et al., 1996; Urbanus et al., 2009). Once in the nucleus these proteins can then bind to their respective DNA targets. DNA-binding by the A-, B-, C-, and E-class proteins is also dependent upon dimerization. *In vitro* analyses of the DNA-binding activity of different combinations of A-, B-, C-, and E-class proteins show that the majority of these floral MADS-box proteins have the ability to bind DNA as homodimers (Huang et al., 1993; Riechmann et al., 1996; West et al., 1998). B-class proteins do not, however, fall into this category. Neither of *Antirrhinum's* two B-class proteins (DEFICIENS and GLOBOSA), nor their respective orthologs in *Arabidopsis* (APETALA3 and PISTILLATA) can bind DNA as homodimers. These proteins can, however, bind DNA when they form heterodimeric complexes with their respective B-class partner; DEFICIENS (DEF) with GLOBOSA (GLO) and APETALA3 (AP3) with PISTILLATA (PI) (Egea-Cortines et al., 1999; Riechmann et al., 1996; Schwarz-Sommer et al., 1992).

Conversion of leaves into floral organs does not occur in plants with ectopic C-class gene expression nor in plants with ectopic expression of both B-class genes, suggesting that dimerization of the MIKC-type MADS-box genes is not sufficient for specification of floral organ identity (Krizek and Meyerowitz, 1996a; Mizukami and Ma, 1992). Further insight into

how this specification of floral organ identity might be accomplished came through the discovery that A-, B-, and C-class proteins can associate with each other in higher-order protein complexes when coexpressed with E-class proteins. These higher-order complexes were shown to enhance protein binding to DNA targets (Egea-Cortines et al., 1999) and to be necessary and sufficient for specification of floral organ identity (Honma and Goto, 2001). These findings led to the development of the 'quartet model' which links specification of floral organ identity to the action of specific tetrameric complexes of A-, B-, C-, and E-class proteins (Theissen and Saedler, 2001). Interestingly, incorporation of DEF/AP3 or GLO/PI proteins into these tetramers requires that first they are bound to one another as a heterodimer (Honma and Goto, 2001; Theissen and Saedler, 2001).

**Autoregulation by B-class heterodimers**

Because B-class function in *Antirrhinum* and *Arabidopsis* requires DEF/AP3 and GLO/PI protein heterodimerization, null mutations in either of the *DEF/AP3* or *GLO/PI* genes result in an identical loss of B-function phenotype (i.e. homeotic conversion of whorl 2 petals into sepals and whorl 3 stamens into carpels) (Bowman et al., 1991; Schwarz-Sommer et al., 1992; Trobner et al., 1992). Null mutation in either of these B-class genes also results in an unexpected down-regulation of its non-mutated partner (Goto and Meyerowitz, 1994; Jack et al., 1992). Comparative studies of B-class gene expression between *def/ap3* mutants and wild type plants show that *GLO/PI* is expressed at low levels early on in the floral development of both types of plants (Goto and Meyerowitz, 1994; Trobner et al., 1992). During later stages of development, however, there is a drastic comparative reduction in the expression of *GLO/PI* in the *def/ap3* mutants (Goto and Meyerowitz, 1994; Trobner et al., 1992). A similar reduction in *DEF/AP3*

expression is observed at late stages of floral development in *glo/pi* mutants (Hill et al., 1998; Jack et al., 1992; Trobner et al., 1992). These observations suggest that induction of *DEF/AP3* and *GLO/PI* expression is controlled by non-B-class transcription factors. They also suggest that subsequent high levels of B-class expression are maintained via positive autoregulation of *DEF/AP3* and *GLO/PI* by the heterodimer of their protein products.

**Conservation of B-function across the angiosperms**

Phylogenetic reconstructions of B-class genes indicate that *DEF/AP3* and *GLO/PI* represent two distinct gene lineages that are the product of a gene duplication event that occurred in an ancestor of the extant angiosperms between 230 and 290 million years ago (Kim et al., 2004). There is strong preferential retention of both lineages in the angiosperms since all of the angiosperms studied to date have at least one *DEF/AP3*-like gene and one *GLO/PI*-like gene (Kramer et al., 1998). Recent studies of the *DEF/AP3*- and *GLO/PI*-like genes of *Gerbera hybrida* (Broholm et al., 2010), *Nicotiana benthamiana* (Geuten and Irish, 2010), *Solanum lycopersicum* (Geuten and Irish, 2010), and *Petunia hybrida* (Vandenbussche et al., 2004) have been instrumental in assessing conservation of B-class function across the angiosperms. B-class function in each of these species is complicated by multiple gene duplications in each of their respective *DEF/AP3* and *GLO/PI* lineages. As a consequence of these duplications all four species have multiple DEF/AP3-like genes, and all but *G. hybrida* have multiple *GLO/PI*-like genes. Within each species there is evidence for some degree of functional redundancy and some degree of subfunctionalization in the duplicated members of both of these lineages. Thus, with one exception, knockouts of individual *DEF/AP3*- or *GLO/PI*-like genes do not result in full homeotic conversion of petals and stamens. Combined knockout or knockdown of all of the

*DEF/AP3*-like genes or all of the *GLO/PI*-like genes of these species does, however, result in full conversion of petals and stamens (Broholm et al., 2010; Geuten and Irish, 2010; Vandenbussche et al., 2004). These results indicate that B-function in these species is specified by the redundant activity of several duplicated *DEF/AP3*-like and *GLO/PI*-like genes. Results from B-class gene expression analyses in these species also indicate a pivotal role for heterodimeric combinations of DEF/AP3-like proteins with GLO/PI-like proteins in the autoregulation of the duplicate *DEF/AP3*- and *GLO/PI*-like genes (Geuten and Irish, 2010; Vandenbussche et al., 2004). This provides compelling evidence that B-class function at the phenotypic and molecular level is highly conserved among the eudicots.

Studies of B-class genes in the monocots indicate that eudicot-like B-function is conserved across the angiosperms (Ambrose et al., 2000; Munster et al., 2001; Nagasawa et al., 2003; Park et al., 2004; Park et al., 2003; Song et al., 2010; Whipple et al., 2004; Whipple et al., 2007; Yao et al., 2008). The monocots are a monophyletic lineage that is distantly related to the eudicots having diverged from the lineage leading to the extant eudicots between 123 and 150 million years ago (Bell et al., 2010; Chaw et al., 2004). The monocots contain approximately one-quarter of all of the known angiosperm species (Joppa et al., 2011). Many of these species have highly derived floral morphologies. Species from the *Poaceae* (grass) family, for example, produce flowers that lack clear sepals and petals. These reduced grass flowers, or florets, develop bract-like organs called the lemma and palea in the floral whorl usually occupied by sepals. In the position of petals grasses develop small, translucent, scale-like organs known as lodicules. Interest in the development of these unique floral organs has led to the isolation and characterization of B-class genes from several Poaceae species (Ambrose et al., 2000; Chung et al., 1995; Hama et al., 2004; Moon et al., 1999; Munster et al., 2001; Whipple et al., 2007). In

all of the Poaceae species studied to date there is a single ortholog of *DEF/AP3* (Munster et al., 2001; Whipple et al., 2007). Loss of function in the *DEF/AP3* ortholog of *Oryza sativa* (rice) and *Zea mays* (maize) (*SUPERWOMAN1* and *Silky1* respectively) results in homeotic conversion of lodicules into lemma/palea-like organs and stamens into carpels (Nagasawa et al., 2003; Ambrose et al., 2000). The Poaceae do, however, have multiple orthologs of *GLO/PI*, which comprise two paralogous *GLO/PI*-like clades. These clades, referred to hereafter as *GLO/PI1* and *GLO/PI2*, are the result of a *GLO/PI* duplication event that occurred sometime between 80 and 61 million years ago before the radiation of the extant Poaceae (Paterson et al., 2004; Vicentini et al., 2008; Whipple et al., 2007). Rice and maize each have one *GLO/PI1*-like gene known respectively as *OsMADS2* and *Zmm16*. There is only one GLO/PI2-like gene in rice (*OsMADS4*), however, two tandem duplicated GLO/PI2-like genes are present in maize (*Zmm18* and *Zmm29*) (Munster et al., 2001; Whipple et al., 2007). While none of these PI/GLO-like proteins were able to homodimerize, all of them had the ability to form heterodimers with their respective DEF/AP3-like partners (Whipple et al., 2004; Yao et al., 2008). These results suggest that B-class function at the molecular level is conserved between eudicots and the monocotolydenous grasses. Some work has also been done to determine the genetic function of Poaceae *GLO/PI*-like orthologs. RNAi knockdown of *OsMADS2* and *OsMADS4* suggest that these genes have unequally redundant B-class functions. Both genes have redundant roles in the specification of stamen identity but *OsMADS4* is relatively less involved than *OsMADS2* in the specification of the lodicules (Yao et al., 2008). The results of this study are not entirely conclusive, however, due to potential off-target effects that are often associated with RNAi transgenes (Li et al., 2011; Senthil-Kumar and Mysore, 2011). To date no loss of function allele has been described for any of the *GLO/PI*-like orthologs in the Poaceae. Here we describe the

functional characterization of the maize S*terile tassel silky ear1* (*Sts1*) gene. We show that this gene is *Zmm16* and that it has B-class function. Our results indicate that expression of this gene is required for proper specification of lodicule and stamen identity, and that this gene is involved in obligate heterodimer-mediated autoregulation of all four of the maize B-class genes.

## B-class genes and sex determination

Results from this study indicate that B class function acts upstream of the maize sex determination process. Maize is a monoecious species in which male florets develop in the apical inflorescence of the plant, known as the tassel, while female florets develop in lateral inflorescences called ears. At early stages of floral development tassel and ear florets are bisexual. At these stages both kinds of florets have a lemma, a palea, two lodicules, three stamens, and a single central gynoecium (Cheng et al., 1983). As development progresses, however, tassel florets and ear florets become unisexual via selective abortion of organs of the inappropriate sex (carpel abortion in the tassel and stamen abortion in the ear) (Cheng et al., 1983). Tassel and ear florets also begin to differ in glume morphology and lodicule development. At maturity male tassel florets have a lemma and a palea, two scale-like lodicules, and three stamens. These florets are encompassed by two large photosynthetic glumes. Ear florets have non-photosynthetic glumes, a lemma, and a palea that all tend to be smaller than those found in the florets of the tassel. Female florets also lack lodicules and stamens but they do have a gynoecium, or fused carpels, in their innermost whorl. Each gynoecium has a long style known as a silk (see Dellaporta and Calderonurrea, 1994 for review).

Studies have shown that sex determination in maize is controlled by the interaction of several sex determination genes, hormones, and environmental factors (see Dellaporta and

Calderonurrea, 1994; Irish, 1996 for reviews). Significant progress has been made in understanding the genetic mechanisms of sex determination via study of various masculinizing and feminizing mutations. *anther ear1*, *dwarf1*, *dwarf2*, *dwarf3*, *dwarf5*, *Dwarf8*, and *Dwarf9* mutants all fail to abort stamens in the florets of the ear (see Dellaporta and Calderonurrea, 1994; Irish, 1996 for reviews). These masculinizing mutations are all associated with defects in the biosynthesis or reception of the plant hormone gibberellin and consequent low levels of gibberellin throughout the plant (Bensen et al., 1995; Cassani et al., 2009; Hedden and Phinney, 1979; Phinney and Spray, 1982; Spray et al., 1996; Winkler and Freeling, 1994; Winkler and Helentjaris, 1995). This suggests that gibberellin plays an important role in wild-type stamen arrest in the florets of the ear. Several mutations that perturb the process of carpel abortion have also been identified (Emerson et al., 1935; Nickerson and Dale, 1955; Phipps, 1928). Feminization of the tassel florets in these *tasselseed* (*ts*) mutants is due to lack of gynoecial abortion and concomitant arrest of the stamens. Glumes and lodicules are also completely feminized in the tassels of at least two of the *ts* mutants (see Dellaporta and Calderonurrea, 1994; Irish, 1996 for reviews). Studies of *ts1* and *ts2* show that these genes play a role in the biosynthesis of a plant hormone known as Jasmonic acid (Acosta et al., 2009). Jasmonic acid, therefore, is important in carpel abortion and in the acquisition of male secondary sex traits in florets of the tassel.

Grassy tillers1 (*Gt1*) is also involved in tassel specific suppression of carpel growth (Whipple et al., 2011). *Gt1* does not, however, seem to be involved in the development of secondary sex traits. Tassel florets of *gt1* mutants frequently have carpelloid outgrowths in their innermost whorl. While these outgrowths occasionally produce silks, they are always infertile. In all other ways *gt1* tassel florets are morphologically wild-type (Whipple et al., 2011). The

role of *Gt1* in carpel abortion is currently unknown. It is likely, however, given *Gt1*'s role in suppression of lateral bud outgrowth (Whipple et al., 2011), that *Gt1* inhibits carpel growth either before or in parallel with the *Tasselseed*-mediated gynoecial abortion process. Our data suggest that *Sts1* acts upstream of the sex determination pathway, and that organ abortion in male florets is specific to organs with carpel identity independent of their position in the flower.

**MATERIALS AND METHODS**

**Genetic stocks**

*sts1-1* was isolated from a forward genetic screen for floral mutants. The M2 plants used in this screen were generated via ethyl mehanesulfonate treatment (EMS) of A619 maize inbreds and subsequent selfing of the resultant M1 plants (Neuffer, 1994). *sts1-2* was isolated from a screen for noncomplementation with *sts1-1*. The 4,000 M1 plants used in this screen were generated via pollination of *sts1-1* ears with EMS mutagenized pollen (Neuffer, 1994) from a different maize inbred, Mo17. *gt1-1* was also isolated from a screen of EMS treated A619 M2s (Whipple et al., 2011). *silky1-mum2* (*si1-mum2*) was provided by Robert Schmidt who isolated it from a maize line with active *Mutator* transposons (Ambrose et al., 2000). *ts1* was provided by Jane Dorweiler who obtained it from the Maize GDB stock center.

The *Zmm16-YFP* transgene was created by in-frame fusion of *YFP* to the C-terminus of *Zmm16* sequence using the Multisite Gateway Three Fragment System (Invitrogen, Carlsbad, CA, USA). This transgene, consisting of 4 kb of the native *Zmm16* promoter, all of the *Zmm16* genomic sequence, and the 3' *YFP* fusion, was then cloned into pTF101.1gw1, a Gateway version of pTF101.1 (Paz et al., 2004). Transference of this plasmid/transgene into Hi Type II

hybrid embryos was performed by the Iowa State University plant transformation facility via *Agrobacteria tumefaciens*-mediated transformation (Frame et al., 2002).

**Double mutants**

  *ts1 sts1* double mutants were generated by crossing *ts1* plants to *sts1-1* homozygotes. Resultant F1s were grown to maturity and selfed.  F2 plants were also grown to maturity and then screened for feminization of the tassel, a phenotype indicative of *ts1* homozygosity.  Plants showing tassel feminization were then genotyped for *sts1-1*.

  *gt1 sts1* double mutants were created by crossing *gt1-1* plants to *sts1-1* homozygotes. Resultant F1s were grown to maturity and selfed.  F2 plants were also grown to maturity and then screened for the tillering phenotype of *gt1-1* mutants.  These tillering mutants were then genotyped for *sts1-1*.

**Genotyping**

  *Sts1* sequence spanning the site of the EMS induced *sts1-1* mutation was amplified via PCR using Sts1-CAPS-For and Sts1-CAPS-Rev as primers (Table 1).  Resulting amplicons were then digested using BPU10I and separated on a 1% agarose gel. Wild-type *Sts1* amplicons are cut once by BPU10I.  The resulting fragments are 224 and 556 bp in length.  *sts1-1* amplicons are not, however, cut by BPU10I.  Uncut *sts1-1* amplicons are 780 bp long.  In plants containing *Sts1-YFP* transgenes, endogenous *Sts1* sequence was amplified using Sts1-CAPS-For and Sts1-CAPS-Rev1 as primers (Table 1).  Sts1-CAPS-Rev1 spans sequence that is interrupted in *Sts1-YFP* transgenes by insertion of *YFP*.  Consequently, there is no amplification of *Sts1-YFP* in PCRs that use these two primers.  Following PCR the amplicons of endogenous *Sts1* are digested

using BPU10I and separated on a 1% agarose gel.  Wild-type *Sts1* amplicons from these PCRs are cut twice by BPU10I.  Resulting fragments are 180, 557, and 787 bp long.  *sts1-1* amplicons from these PCRs are cut once by BPU10I.  The fragments are created by digestion of this allele are 180 bp and 1344 bp long.

*Sts1-YFP* transgenes were detected via leaf treatment with glufosinate-ammonium. Finale® Weed and Grass Killer with 5.78% glufosinate-ammonium was diluted in water (one part Finale® to ninety nine parts water).  This diluted weed killer was then applied to the ad- and abaxial surfaces of a mature maize leaf using a Q-tip®.  The sections of the leaves treated with weed killer were approximately 4 cm long and were marked previous to Finale® treatment using a permanent marker.  The leaves were checked daily for one week after treatment for signs of chlorosis and desiccation.  Because the plasmid carrying the *Sts-YFP* transgene also carries a *bar* gene, which confers glufosinate-ammonium resistance, the leaves of *Sts-YFP* transgenic plants are unaffected by Finale® treatment.  The leaves of plants that lack the *Sts-YFP* transgene, however, experience noticeable chlorosis and desiccation during the one week observation period following Finale® application.

*Gt1* sequence spanning the site of the EMS induced *gt1-1* mutation was amplified using Gt1-CAPS-For and Gt1-CAPS-Rev (Table 1) and digested with BsaJI according to the *gt1* genotyping protocol described by Whipple et al. (2011).

Wild-type *Silky1* (*Si1*) sequence was amplified by PCR using primers Si1-For and Si1-R (Table 1).  Because these primers anneal to DNA sequence on either side of the *Mutator* transposon insertion site associated with *si1-mum2* they do not amplify *si1-mum2* sequence.  In a separate reaction *si1-mum2* sequence was amplified by PCR using Si1-For and Mu-TIR6 (Table

1).  The Si1-For and Mu-TIR6 primer pair will not amplify Wild-type sequence because the Mu-TIR6 primer is specific to the *Mutator* transposon.

**Scanning electron microscopy**

Inflorescences were fixed in freshly prepared FAA (3.7% formaldehyde, 5% acetic acid, 50% ethanol) for 16 hours or more.  Following fixation they were washed with 35% ethanol and 15% ethanol.  They were then washed 3 times with 0.1 M sodium cacodylate buffer and post-fixed for 4 hrs in 1% osmium tetroxide in 0.1M sodium cacodylate.  Following post-fixation, the samples were rinsed six times with $dH_2O$.  They were then dehydrated through a graded ethanol series (starting with 10% ethanol, and then progressing through 30% ethanol, 50% ethanol, 70% ethanol, 95% ethanol, and 100% ethanol) and dried with a critical point drier.  These dried samples were then mounted, dissected, sputter coated with gold palladium, and viewed at 10 kV accelerating voltage with a FEI XL30 environmental scanning electron microscope.

**RNA *in situ* hybridization**

Wild-type and *sts1-1* inflorescences were fixed overnight at 4°C in 4% in para-formaldehyde in 1X PBS.  These fixed samples were then dehydrated in ethanol, transitioned into Histo-Clear® (National Diagnostics, Atlanta, GA, USA), embedded in paraplast, sectioned, and hybridized according to the protocol previously described by Jackson et al. (1994).  All hybridizations were performed using the *Gt1* antisense digoxygenin-labeled RNA probe described by Whipple et al. (2011).

**qRT-PCR expression analysis**

Total RNA was extracted from three developmental stages of male inflorescences from *st1-1*, *si1-mum2*, and wild-type plants. Inflorescence branches of approximately 1 cm long were considered stage 1. Because maize spikelets mature acropetally, with the most advanced spikelets at the base of the inflorescence, and because their associated florets mature basipetally, stage 1 inflorescences contain florets from a variety of developmental stages. The most advanced florets of stage 1 inflorescences do, however, still represent a relatively early stage of floral organ development in which lodicule primordia are just beginning to initiate (comparable to stage G in Cheng et al., 1983). Stamens in these florets have a bulbous morphology and have not yet attained the tetralocular or flattened form typical of the stamens in older florets. 2.5 cm long central spikes were chosen to represent stage 2. The majority of florets from these spikes were of later developmental stages than the florets of their corresponding stage 1 branches. The most advanced florets of these inflorescences have lodicules that are fully initiated, stamens that are tetralocular or flattened, and a gynoecium with a distinctive gynoecial ridge (comparable to stage H or I in Cheng et al., 1983). Stage 3 was represented by unopened spikelets that were collected from recently emerged tassels (comparable to stage J in Cheng et al., 1983). RNA was extracted from these tissues using TRI reagent (Sigma-Aldrich, St. Louis, MO, USA) and the Qiagen RNeasy® Plant Mini Kit (Qiagen, Valencia, CA, USA) as follows: Inflorescences/florets were ground in liquid nitrogen using a mortar and pestle, 1 mL of TRI reagent was then added to the ground tissue, and the tissue-TRI reagent mixture was transferred to a 2 mL microcentrifuge tube. 200 µL of chloroform was added, the mixture was vortexed, and then centrifuged at 15,000 xg for 10 min. 200 µL of the resulting supernatant was added to 700 µL of Qiagen RLT buffer, 500 µL 100% ethanol was then added to the mixture, which was

subsequently mixed by vortexing.  This mixture was added to a RNeasy Mini Spin Column and purified following a modified version of the RNeasy® Plant Mini Kit protocol.  Modifications were as follows: 1) Exclusion of the RW1 buffer wash step.  2) Two washes with 750 µL of 80% ethanol following a single RPE buffer wash.  3) Final elutions with 11µL of RNase free water instead of with 30-50 µL of RNase free water.  Resulting RNA samples were treated with DNase (Promega, Madison, WI, USA) following manufacturer's protocol.  DNased RNA was then reverse transcribed using an oligo-dT primer and SuperScript$^{TM}$ III RT (Invitrogen) according to manufacturer's protocol.  The amount of 25 mM $MgCl_2$ added to the RT reaction was reduced from 4 to 2 µl to account for carry over Mg from the DNase reaction.

*Sts1*, *Si1*, and *Zmm18/29* expression was analyzed by quantitative PCR (qPCR) of cDNA from the previously mentioned wild-type and mutant inflorescences.  TaqMan® chemistry was chosen for these qPCR analyses to ensure that detection of amplification would be specific to each individual target gene.  We also ensured that gDNA would not be amplified during these reactions by designing primers that spanned exon-exon junctions.  The cDNA-specificity of these primers was confirmed by conventional PCR tests.  These tests showed high levels of PCR amplification in reactions containing cDNA templates and no amplification in reactions containing gDNA templates (data not shown).  Because of extremely high cDNA sequence similarity and probable functional redundancy between *Zmm18* and *Zmm29* (Munster et al., 2001; Whipple et al., 2004) we chose to assay the composite expression of these two genes.  The primers and probes used in this study do not, therefore, distinguish between *Zmm18* and *Zmm29*. The primers and probes for these genes, *Sts1*, *Si1*, and the endogenous α*Tubulin* control use in qPCRs are listed in table 2.

qPCR was performed on a StepOnePlus^TM Real-Time PCR machine using the TaqMan® Gene Expression Master Mix (Applied Biosystems, Foster City, CA, USA). Reaction volumes were 20 µL and consisted of 10 µL of TaqMan® Gene Expression Master Mix, 2 µL of 6 µM forward primer, 2 µL of 6 µM reverse primer, 2 µL of 2.5 µM TaqMan® probe, 2 µL of molecular grade $H_2O$, and 2 µL of 50 ng/µL cDNA. Each reaction was performed in triplicate under the following conditions: 50ºC for 2 min, 95ºC for 10 min, and 40 cycles of two step amplification (95ºC for 15 sec followed by 60ºC for 1 min). Each reaction plate assayed the expression of all three of the B-class genes and the endogenous α*Tubulin* control gene in three wild-type biological replicates and three mutant biological replicates. No-RT controls were also included in these plates. ΔCt, ΔΔCt, and standard deviations for each biological replicate (the combination of the three technical replicates) and for each biological group (the combination of the three biological replicates) were calculated by the StepOne^TM software v2.2.2. Analysis of significance was performed on ΔΔCt values using the two tailed student's t test. Average fold change was determined using the $2^{\wedge\Delta\Delta Ct}$ method (Livak and Schmittgen, 2001) and fold change range was determined via $2^{\wedge\Delta\Delta Ct + SD}$ and $2^{\wedge\Delta\Delta Ct - SD}$.

**RESULTS**

**Characterization of the *sts1* phenotype**

The *sts1* mutant was discovered in a forward genetic screen for mutations affecting the tassel floret. *sts1* tassel florets are sterile due to homeotic conversion of their stamens into bract-like structures resembling the lemma and the palea. Lodicules in these mutants are likewise transformed into similar lemma/palea-like organs (Figure 1B). *sts1* mutants have no distinctive vegetative phenotype. Their ears, however, have a noticeably higher density of silks than do the

ears of their wild-type counterparts (Compare Figure 2A to 2D). This higher silk-density is due to the formation of extra carpels in the florets of *sts1* ears. The number of extra carpels varies among these florets, with some having one extra carpel and others having two or three. Regardless of number, however, these additional carpels were always found in regions of the floret typically occupied by arrested stamens. This suggests that the stamens of *sts1* ear florets are homeotic conversion into carpels (Figures 2E,F).

**Characterization of the *si1* phenotype**

The *si1-mum2* tassel floret phenotype is identical to that of *sts1*. Tassel florets from these mutants develop wild-type lemmas and paleas in their first whorl. The lodicules (whorl 2) and stamens (whorl 3) of these mutants are homeotically transformed into lemma/palea-like organs (Figure 1C). Loss of function in *Si1* has no further effect on tassel or vegetative morphology. The central gynoecium of *si1-mum2* ear florets is surrounded by addition carpels that arise in the regions of whorl 3 typically occupied by the stamens. As in *sts1*, the number of additional carpels found in these ears varies between florets. Fusion of these extra carpels to the central gynoecium was common in ear florets of *si1-mum2* (Figures 2G,H).

**Early development of the *sts1* mutant**

In order to more fully understand how floret development differs between wild-type and *sts1* plants scanning electron microscopy was used to analyze a comparative developmental series of young wild-type and *sts1* florets. At very early stages in tassel floret development, shortly after initiation of the lemma, *sts1* and wild-type floral meristems both form a primordial ridge that eventually becomes the palea. Following initiation of the palea primordia wild-type

and mutant florets also form three bulbous stamen primordia (Figures 3A and 3C). During subsequent development, the stamens of wild-type plants begin to assume a distinctive tetralocular form. This is not the case for organs in this position of *sts1* mutants, however. Instead of becoming tetralocular, these organs become ab/adaxially flattened (Compare Figures 3B and 4A to Figures 3D and 4C). During this stage of development ectopic primordia initiate in the axils of the transformed stamens of many *sts1* florets. The number and position of these ectopic primordia did vary, however, with a few mutant florets lacking ectopic primordia, many containing a single ectopic primordium in the axil of the medial transformed stamen, and others containing two ectopic primordia in the axils of both of the lateral transformed stamens (Figures 3D and 4C).

s*ts1* initiation of lodicule primordia is comparable to lodicule initiation in wild-type plants (Figures 3B and 3D). After initiation, wild-type lodicules become compact and scale-like while the transformed lodicules of *sts1* florets become flattened in a manner similar to that observed in transformed *sts1* stamens. The transformed stamens and lodicules develop an increasingly broad and elongated morphology ultimately resembling the lemma and the palea (Figures 4B-D).

**Genetic characterization of *sts1***

The s*ts1* mutant was crossed to B73 and the resulting F1s were selfed to generate an F2 mapping population. Coarse mapping was accomplished via bulk-segregate analysis (Michelmore et al., 1991) of F2s from this cross. The results of this mapping localized *sts1* to chromosome 3 (complete linkage, 0/X chromosomes, with the SSR marker *umc1266*). The B-class gene *Zmm16* is 3.39 Mb distal to *umc1266* and was a likely candidate. Sequences of

*Zmm16* from wild-type and *sts1* plants were compared, and a putative EMS-induced mutation was identified in the sequence corresponding to the *sts1* mutant. This mutation, a G to A base transition, is found in the donor site of the third intron of this gene (C. Whipple, unpublished data) (Figure 5). To confirm that *sts1* and *Zmm16* are in fact the same gene, a second EMS-induced allele of *sts1* was generated. This second allele, referred to hereafter as *sts1-2* was identified by a non-complementation screen and is also associated with an EMS-induced mutation in *Zmm16*. Unlike *sts1-1*, however, the G to A base change associated with *sts1-2* is found in the splice acceptor site of intron four (Figure 5).

To further confirm that the *sts1* phenotype is caused by mutations in *Zmm16,* we performed a phenotypic rescue experiment using a *Zmm16-YFP* transgene. Analysis of YFP signal in plants containing this transgene show that *Zmm16-YFP* recapitulates the known expression pattern of endogenous *Zmm16* (S. Deblasio, unpublished data; Munster et al., 2001). In our rescue experiment, *Zmm16-YFP* transgenic plants were crossed to *sts1-1* mutants. Resulting progeny were grown to maturity and scored for the presence of the transgene. Plants containing the transgene were then selfed. F2's from these selfings were also grown to maturity, genotyped for *sts1* homozygotes, scored for the presence of the transgene, and scored for the presence or absence of the *sts1* phenotype. Of the 11 F2 *sts1-1* homozygotes identified in this experiment, 6 scored positive for the presence of the transgene. All 6 of these transgenic *sts1-1* homozygotes had wild-type floret phenotypes suggesting full rescue of the *sts1* phenotype by *Zmm16-YFP* (Table 3).

**Expression of the B-class genes in *sts1* and *si1* mutants**

To determine whether the B-class genes of maize are involved in positive autoregulation we examined the expression of *Sts1*, *Si1*, and *Zmm18/29* in *sts1-1* mutants, *si1-mum2* mutants, and wild-type plants. Expression of these genes was analyzed by quantitative reverse transcription PCR (qRT-PCR) on cDNA isolated from a developmental series of tassel inflorescences from these plants. At early stages of development (stage 1) there is a slight decrease in the expression of *Si1* (1.5 fold) in *sts1-1* plants compared to wild-type. Differential expression of *Si1* between *sts1-1* and wild-type becomes more pronounced at later stages of development (stage 2 and stage 3). At stage 2 *sts1-1* plants have a 2.1 fold decrease in *Si1* expression compared to wild-type, and at stage 3 they have a 12.8 fold comparative decrease in *Si1* expression (Figure 6A). *Zmm18/29* expression in stage 1 *sts1-1* is decreased relative to wild type significantly more (9.3 fold) than was *Si1*. Relative expression of *Zmm18/29* in later stages of *sts1-1* plants is decreased at higher levels than it is at this initial stage (stage 2 plants have a 15.3 fold decrease, stage 3 plants have a 14 fold decrease) (Figure 6A). Fold change decreases of *Zmm18/29* in *sts1-1* mutants are not significantly different at stages 2 and 3. Expression of *Sts1-1* itself is also decreased in *sts1-1* mutants relative to wild-type. This decrease is present at all stages of development with stage 1 *sts1-1* inflorescences showing a 2.1 fold decrease, stage 2 inflorescences showing a 5 fold decrease, and stage 3 inflorescences showing a 17 fold decrease relative to wild-type (Figure 6A).

In *si1-mum2* mutants, *Si1* transcripts were present at such low levels that their expression relative to wild-type is not included (Figure 6B). At stage 1 *Sts1* expression is decreased 1.2 fold in *si1-mum2* plants relative to wild-type. This value was the only fold change value from our study that was not, however, significant at P<0.05. Relative fold change decreases in *Sts1* expression were much higher in *si1-mum2* inflorescences at stage 2 (11.6 fold) and stage 3

(811.8 fold) (Figure 6B). There is also a higher initial decrease in the expression *Zmm18/29* (20.6 fold) in stage 1 *si1-mum2* plants relative to wild type than there is in the expression of *Sts1*. *Zmm18/29* expression in stage 2 is decreased by 161.6 fold relative to wild-type and it is decreased by 692.8 fold in stage 3 (Figure 6B).

These qRT-PCR results show a general trend of decreasing B-class gene expression in the B-class mutants relative to wild-type. With each successive stage of development there is a progressive decrease in the relative expression of B-class genes in *sts1-1* and *si1-mum2* mutant inflorescences. Generally, these decreases in B-class gene expression relative to wild-type appear to be higher in *si1-mum2* mutants than they are in *sts1-1* mutants.


**Characterization of *ts1 sts1* and *gt1 sts1* double mutants**

Because the stamens of *sts1* tassel florets are converted into lemma/palea-like organs while the stamens of corresponding ear florets are converted into carpels we hypothesized that lack of stamen-to-carpel conversion is due to tassel-specific carpel abortion by the male sex determination pathway. To test this, we generated double mutants between *sts1-1* and *ts1*. *ts1* was chosen for this study because of its well characterized role in the control of male sex determination (Acosta et al., 2009). *ts1* single mutants have feminized tassel florets that contain a fertile gynoecium in their central whorl. The *ts1* mutation also causes abortion of the stamens and affects secondary sexual traits. *ts1* tassel florets, therefore, lack stamens and lodicules, and have reduced glumes (Figures 7A, B). *ts1 sts1-1* double mutant tassel florets also have these secondary female traits and a fertile central gynoecium. In addition they have carpels that form in the regions of whorl 3 typically occupied by arrested stamens (Figures 7C,D).

To control for secondary sexual characters we also made *gt1-1 sts1-1* double mutants. Tassel florets of *gt1-1* single mutants frequently contain carpelloid outgrowths in their central whorl. In all other aspects *gt1-1* tassel florets are morphologically wild-type (Figure 8A). *gt1-1 sts1-1* tassel florets are similar to *sts1-1* florets in that their lodicules are transformed into lemma/palea-like organs. The stamens of these double mutant florets have varying degrees of carpelloidy. Many are lemma/palea-like with carpelloid tissue at their base and others produced silks. None of the transformed stamens of these double mutants had full carpel identity, however. This suggests that there are other genes involved in carpel suppression/abortion that act redundantly with *Gt1* in the sex determination pathway.

### *Gt1* expression in *sts1* mutants

To further understand suppression of carpel growth in the transformed stamens of *sts1* tassels we observed expression of *Gt1* in *sts1-1* plants expecting to see *Gt1* expression in transformed third whorl stamens. Expression of *Gt1* in mutant tassel florets was determined using *in situ* RNA hybridization. Inflorescences used in this analysis had florets of developmental stages comparable to stages F-H described in Cheng et al. (1983). At early stages of development, before formation of a gynoecial ridge on the central gynoecium, *Gt1* expression was not detected anywhere in the floret (data not shown). After formation of the gynoecial ridge strong *Gt1* expression was detected in central carpel primordia (Figures 9A,B). *Gt1* was not, however, detected in the transformed stamens.

### DISCUSSION

### *Sts1* is *Zmm16*, a maize ortholog of *GLO/PI*

*Sts1* has been identified by mapping EMS-induced *sts1-1* and *sts1-2* mutations to the MIKC-type MADS-box gene, *Zmm16*. Previous studies have shown that *Zmm16* is an ortholog of the eudicot B-class genes *GLO* and *PI* (Munster et al., 2001; Whipple et al., 2004). Proteins from *Zmm16* can interact in vitro with those produced by *Si1*, the maize ortholog of *DEF/AP3* (Whipple et al., 2004). ZMM16 can also interact in vivo with AP3 in a heterodimeric complex capable of rescuing the null *pi* mutant phenotype of *Arabidopsis* (Whipple et al., 2004). These results indicated that *Zmm16* has a B-class function similar to that provided by *GLO* and *PI* in *Antirrhinum* and *Arabidopsis*. The phenotype of *sts1* mutant plants is consistent with this proposed B-class function for *Zmm16*. As is the case for *si1* (Ambrose et al., 2000) and B-class mutants in other species (Bowman et al., 1991; Schwarz-Sommer et al., 1992; Trobner et al., 1992) transformation of floral organ identity in *sts1* is limited to whorls 2 and 3. Rescue of this *sts1* B-class mutant phenotype by the *Zmm16-YFP* transgene provides additional support for the conclusion that *Sts1* is *Zmm16*.

**Organ abortion in the unisexual florets of maize affects the *sts1* mutant phenotype**

The transformed stamens of male and female florets in *sts1* mutants have striking differences in morphology. Where the stamens of female florets are converted into carpels, the stamens of male florets seem to be transformed into lemma/palea-like organs (Compare Figure 1B and 2F). This apparent difference in the identity of transformed stamens in male and female florets has not been reported for *si1* mutants. Rather, stamens in plants homozygous for *si1-R* and *si1-5* are converted into carpelloid organs regardless of the sexuality of the floret from which they arise (Ambrose et al., 2000). Molecular lesions associated with both of these *si1* alleles are still unidentified, however, and it is possible that other alleles of *si1* have a phenotype more

similar to *sts1*. We show that other well-characterized alleles of *si1* (i.e. *si1-mum2*) also cause conversion of male floret stamens into lemma/palea-like organs (Figure 1C). Like *sts1*, the stamens of *si1-mum2* female florets are also transformed into carpels (Figures 2G,H). This suggests that sexual dimorphism in the identity of transformed stamens is normal for B-class gene mutations in maize.

It is likely that lack of stamen-to-carpel conversion in male florets of these mutants is related to the maize sex determination pathway. The primary effect of this sex determination process is the abortion of carpel primordia and stamen primordia early in the development of male and female florets respectively (Dellaporta and Calderonurrea, 1994). This inflorescence specific abortion of carpels and stamens may be organ rather than whorl-specific. If this is indeed the case, any organ with carpel identity in the male florets of maize would be targeted for abortion by the sex determination pathway. This may explain why the transformed stamens of *sts1* and *si1* mutants do not have apparent carpel identity. Transformation of stamens into carpels in *ts1 sts1-1* double mutants suggests that this hypothesis of organ specific abortion is correct. Our results make it clear that B-class gene establishment of floral organ identity acts upstream of the carpel abortion pathway. This is in contrast with a study in *Cucumis sativus* (cucumber) that demonstrated that organ abortion occurs in a whorl specific manner regardless of floral organ identity (Kater et al., 2001). This is not surprising, however, considering that floral unisexuality has evolved independently in various angiosperm lineages (Mitchell and Diggle, 2005; Yampolsky and Yampolsky, 1922). The role that B-class genes play in the establishment of floral unisexuality will vary, therefore, from species to species.

Although the sex determination role of *Gt1* is not yet fully understood, it is likely that this gene inhibits carpel growth early on in floral development prior to carpel abortion mediated by

the *Tasselseed* pathway (Whipple et al., 2011).   Results from our *gt1-1 sts1-1* double mutant study indicate that B-class gene establishment of floral organ identity also acts upstream of *Gt1*. This is evidenced by the fact that the transformed stamens of these double mutants have partial carpel identity (Figure 8B).  These transformed stamens are not, however, fully carpelloid indicating that other genes involved in carpel suppression/abortion are still functional even in the absence of GT1.  Whether these are *Tasselseed* genes or other as-of-yet uncharacterized genes has yet to be determined.

**Sts1 and Si1 are involved in heterodimer-mediated B-class autoregulation**

Eudicot *DEF/AP3*-like and *GLO/PI*-like genes are positively autoregulated by heterodimeric complexes of DEF/AP3-like and GLO/PI-like proteins (Goto and Meyerowitz, 1994; Jack et al., 1992).  To test conservation of this unique autoregulatory mechanism in maize we measured expression of all of the *B*-class genes in wild-type, *sts1-1*, and *si1-mum2* male inflorescences.  At early stages of floral development expression of *Sts1* was comparable in *si1-mum2* mutants, *sts1-1* mutants, and wild-type plants (Figure 6A,B).  This suggest that induction of *Sts1* expression is independent of the SI1-STS1 heterodimer.

At later stages of development *Sts1* is highly down regulated in *sts1-1* and *si1-mum2* mutants relative to wild-type.  *Si1* expression is also similarly down regulated in the *sts1-1* mutants.  These results indicate that *Sts1* and *Si1* both play a role in the maintenance of high levels of B-class gene expression at late stages of floral development.  It is not clear, however, whether this positive B-class autoregulation is direct or indirect.  Insight into the directedness of this autoregulation could be provided via ChIP-sequencing of DNA bound by complexes containing STS-YFP proteins.

Our data also show that *Zmm18/29* expression is low in *sts1-1* and *si1-mum2* mutants relative to wild-type at early stages of development.  This suggests that *Sts1* and *Si1* may be involved in induction of *Zmm18/29* floral expression.  In vitro Binding of SI1-STS1 heterodimers to sequence in the first intron of *Zmm18/29* (data not shown) suggests that this induction may be direct.  This may explain why there is non-redundancy between *Zmm18/29* and *Sts1*.  If expression of *Zmm18/29* were initiated independent of *Sts1* it is possible that these genes would be functionally redundant with Sts1 as is seen in other species with multiple B-class paralogs (Broholm et al., 2010; Geuten and Irish, 2010; Vandenbussche et al., 2004; Yao et al., 2008).

**Sts1 and Zmm18/29 are not fully functionally redundant**

It is surprising considering the highly comparable expression patterns of *Sts1* and *Zmm18/29* and the high sequence similarity of their respective protein (Munster et al., 2001) that mutation in *Sts1* alone causes such a strong B-class phenotype.  This suggests that the function of *Zmm18/29* is not fully redundant with that of *Sts1*.  It is possible that *Zmm18/29* have developed novel functions (neofunctionalized) or that they are functionally redundant with *Sts1* only at late stages of development.  This hypothesis of late stage redundancy is consistent with a model suggesting induction of *Zmm18/29* by the SI1-STS1 heterodimer.  Preliminary analyses of *Zmm18/29* RNAi lines suggest that there is no floral phenotype associated with knockdown of function in these genes (data not shown).  Generation of *sts1 zmm18 zmm19* triple mutants will likely be necessary to accurately determine the function of *Zmm18/29*.

While this study has shown that there is a high degree of conservation in genetic and molecular function of the B-class genes in eudicots and monocots, it is clear that more needs to

be done to determine the fate of duplicate Poaceae *GLO/PI*-like genes.  Functional

characterization of the *GLO/PI*-like genes of rice (*OsMADS2* and *OsMADS4*) indicates that these

genes have subfunctionalized (Yao et al., 2008).  *OsMADS2* is involved in specification of

lodicule and stamen identity while *OsMADS4* seems only to be involved in specification of the

stamens.  Further analysis of *Sts1, Zmm18,* and *Zmm29* will almost certainly shed further light on

the possible neo-, non-, or subfunctionalization of *GLO/PI*-like duplicates.

| Primer Name | Primer Sequence |
|---|---|
| Sts1-CAPS-For | TCG GAT AGG GGA ACA GAC AG |
| Sts1-CAPS-Rev | ATC AGG TCT TTG GGT TGC AG |
| Sts1-CAPS-Rev1 | GCA TCC AGC AGT CTA ATT GT |
| Gt1-CAPS-For | AGG TGG CCG TCT GGT TCC AGA A |
| Gt1-CAPS-Rev | TGG TGC GTC ACC GTC GAG AAC |
| Si1-For | GTG CTG CTG TGC TCA TCA AT |
| Si1-Rev | TAG GTA TCA GTC TGC GTG CTG |
| Mu-TIR6 | AGA GAA GCC AAC GCC AWC GCC TCY ATT TCG TC |

**Table 1.** Genotyping primers for *sts1-1*, *gt1-1*, and *si1-mum2*.

| Primer or Probe Name | Primer or Probe Sequence |
|---|---|
| Sts1-RTPCR-For | ATA ATG GAC TGA CGA ACC TGA ATG |
| Sts1-RTPCR- Rev | GCG ATA TCT TGC TGG TGG AGT |
| Si1-RTPCR- For | CAC AGA GAT TAG GCA AAG GAT GG |
| Si1-RTPCR-Rev | AGT CTG CGT GCT GAT CAC ATG |
| Zmm18/29-RTPCR-For | ATG CAG ATT CAG CTC AGG CAT |
| Zmm18/29-RTPCR-Rev | CAG TAG TCC ATC TGC TTC TCG C |
| αTubulin-RTPCR-For | GAG CAT GGC ATT CAG GCT G |
| αTubulin-RTPCR-Rev | CAA GGT CAA CAA AAA CAG CAC G |
| Sts1-Probe | 6FAM-AAG GCC AGC AAT TTG TTC TCG TCT TCC AT-TAMRA |
| Si1-Probe | 6FAM-ATC TGG ACA GTC TGG ACT TCG ACG AGC T-TAMRA |
| Zmm18/29-Probe | 6FAM-ATG TTG GTC TGC CCA TTC TGG AGG C-TAMRA |
| αTubulin-Probe | 6FAM-CAG ATG CCC GGT GAC AAG ACC ATT G-TAMRA |

**Table 2.** Primers and probes for qRT-PCR of *Sts1, Si1,* and *Zmm18/29*. The primers and probe for qRT-PCR of the α*Tubulin* control are also listed.

| Genotype | *Zmm16-YFP* | Phenotype | Number of Plants |
|---|---|---|---|
| *sts1-1/sts1-1* | Present | wild-type | 6 |
| *sts1-1/sts1-1* | Present | *sts1* | 0 |
| *sts1-1/sts1-1* | Absent | wild-type | 0 |
| *sts1-1/sts1-1* | Absent | *sts1* | 5 |
| *+/sts1-1* | Present | wild-type | 8 |
| *+/sts1-1* | Present | *sts1* | 0 |
| *+/sts1-1* | Absent | wild-type | 8 |
| *+/sts1-1* | Absent | *sts1* | 0 |
| *+/+* | Present | wild-type | 9 |
| *+/+* | Present | *sts1* | 0 |
| *+/+* | Absent | wild-type | 3 |
| *+/+* | Absent | *sts1* | 0 |

**Table 3.** Phenotypic rescue of *sts1-1* by *Zmm16-YFP*.
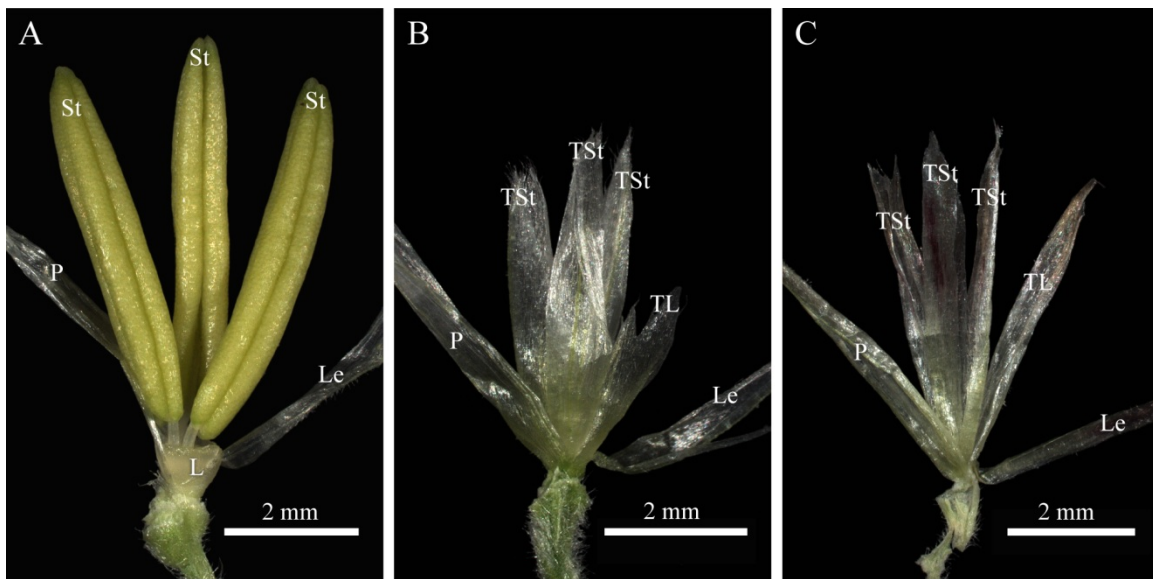


**Figure 1.** Phenotypes of wild-type, *sts1-1*, and *si1-mum2* tassel florets. **(A)** A mature wild-type tassel floret. The lemma (Le) and palea (P) are both visible as is a single lodicule (L) and all of the floret's three stamens (St). **(B)** The mature tassel floret of a *sts1-1* mutant showing transformed stamens (TSt) and a transformed lodicule (TL) enclosed by a phenotypically normal lemma (Le) and palea (P). **(C)** A mature *si1-mum2* tassel floret with lemma (Le) and palea (P) opened up to reveal three transformed stamens (TSt) and one transformed lodicule (TL).
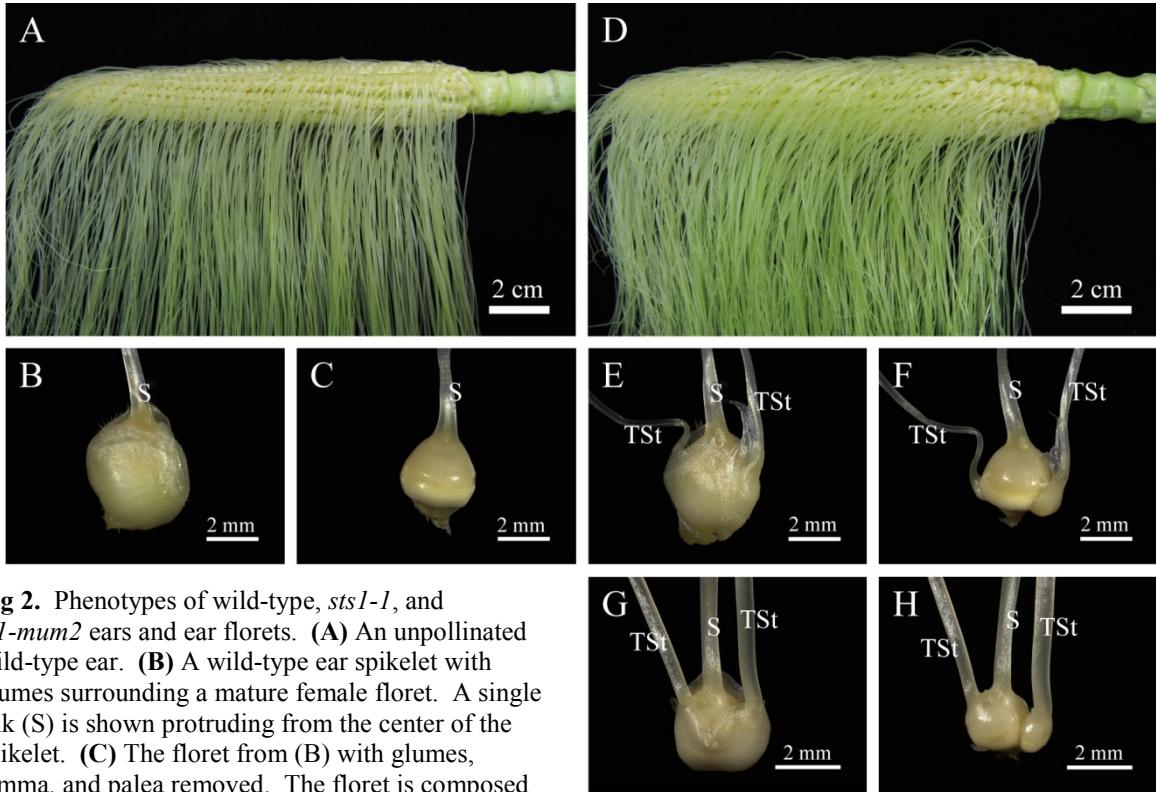
**Fig 2.** Phenotypes of wild-type, *sts1-1*, and *si1-mum2* ears and ear florets. **(A)** An unpollinated wild-type ear. **(B)** A wild-type ear spikelet with glumes surrounding a mature female floret. A single silk (S) is shown protruding from the center of the spikelet. **(C)** The floret from (B) with glumes, lemma, and palea removed. The floret is composed mostly of a large gynoecium and its associated silk (S). **(D)** An unpollinated *sts1-1* mutant ear. **(E)** A *sts1-1* ear spikelet showing protrusion of three silks beyond the glumes. Removal of the glumes, lemma, and palea from (E) reveals **(F)** a single female floret with a central silk (S) flanked on either side by silks associated with two transformed stamens (TSt). **(G)** A *si1-mum2* ear spikelet and its associated floret **(H)**. Both show three silks with two lateral silks coming from transformed stamens (TSt) and the third central silk (S) coming from the gynoecium.

**Figure 3.** SEMs of wild-type and *sts1-1* tassel florets at early stages of development. **(A,B)** Wild-type. **(C,D)** *sts1-1* mutants. **(A,C)** Tassel florets showing stamen primordia (StP) and a single palea primordium (PP). **(B,D)** Young tassel florets with wild-type stamens (St) assuming a tetralocular shape and transformed stamens (TSt) becoming ad/abaxially flattened. Ectopic primordia (*) are shown in the axils of two of the transformed stamens of the *sts1-1* floret at this stage of development. At this stage the lodicules (L) of wild-type florets and transformed lodicules (TL) of *sts1-1* florets are similar in their morphology. The central gynoecium (G) and first whorl palea (P) of wild-type and *sts1-1* florets are also comparable in their morphology.
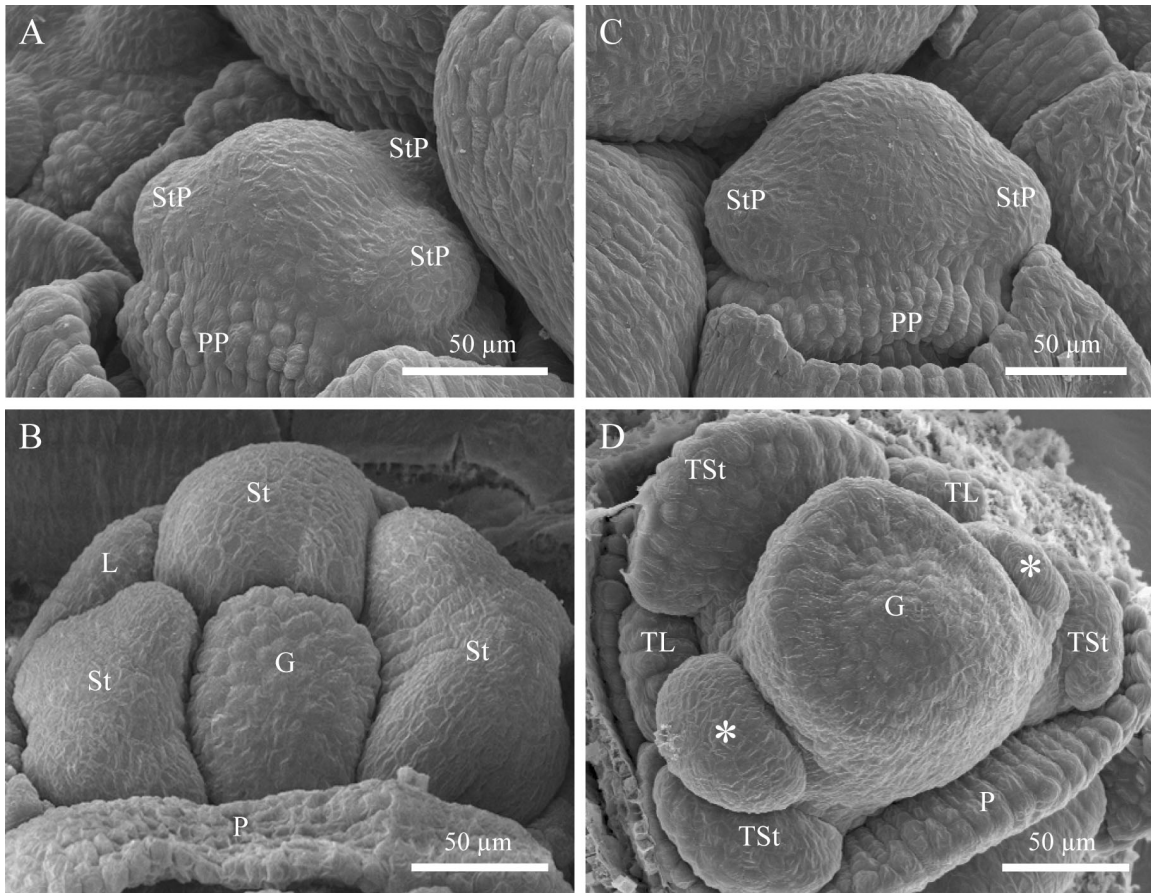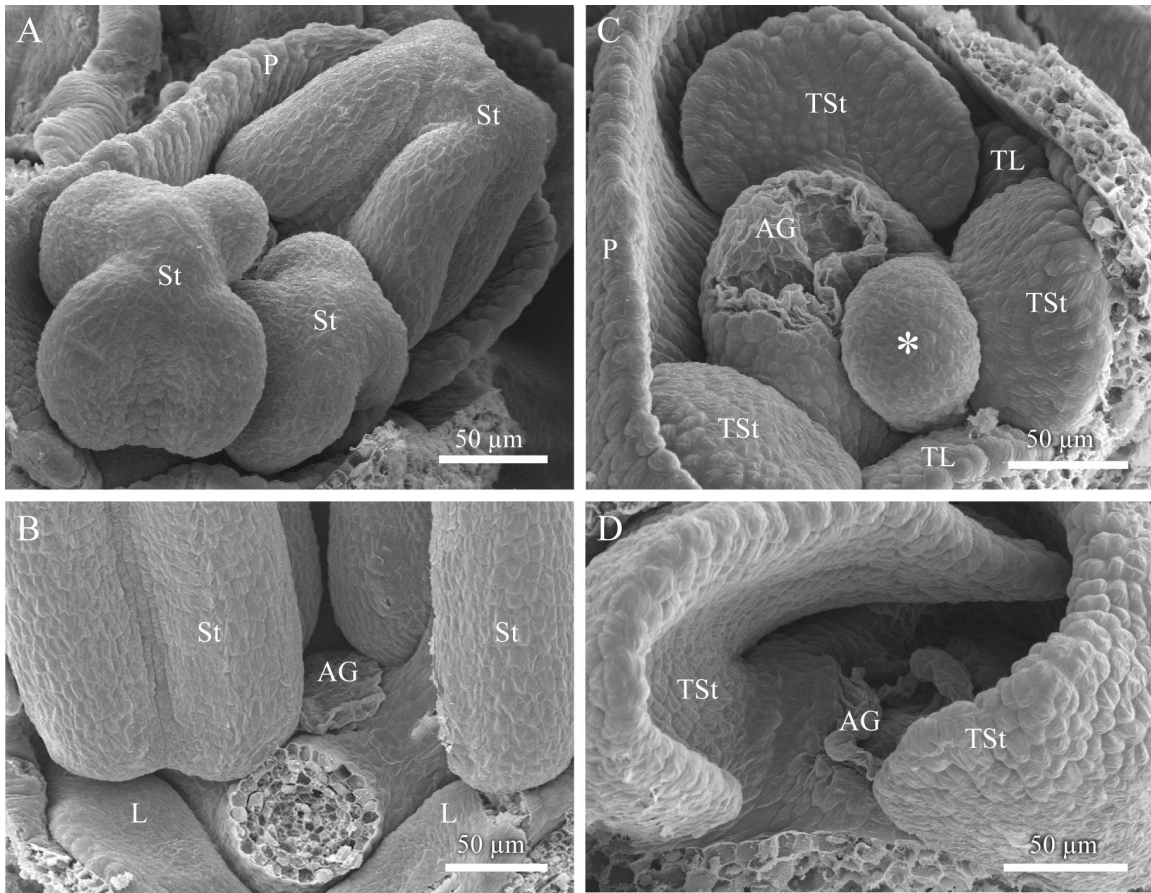
**Figure 4.** SEMs of wild-type and *sts1-1* tassel florets at late stages of development. **(A,B)** Wild-type. **(C,D)** *sts1-1*. **(A,C)** Florets from later stages of development with plump tetralocular wild-type stamens (St) or broad flattened transformed stamens (TSt). One ectopic primordia (*) has formed in the axil of the central transformed stamen of the *sts1-1* floret depicted here. An aborted gynoecium (AG) is visible in the *sts1-1* floret of this stage as are two broad flattened transformed lodicules (TL). The paleas (P) of wild-type and *sts1-1* florets at this stage remain morphologically identical. **(B,D)** Florets from very late stages of development. Two large tetralocular stamens (St) are visible in the wild-type floret and the third stamen has been removed to reveal a central aborted gynoecium (AG) and two compact glandular lodicules (L). Two broad lemma/palea-like transformed stamens (TSt) are visible in the *sts1-1* floret. The third transformed stamen has been removed to reveal the central aborted gynoecium (AG). The transformed lodicules of *sts1-1* florets from this stage of development (not shown) also have a broad lemma/palea-like morphology.

A

sts1-1          sts1-2
G>A             G>A

B

ATG GGG CGC GGC AAG ATC GAG ATC AAG CGG ATC GAG AAC TCC ACC AAC CGC CAG
 M   G   R   G   K   I   E   I   K   R   I   E   N   S   T   N   R   Q

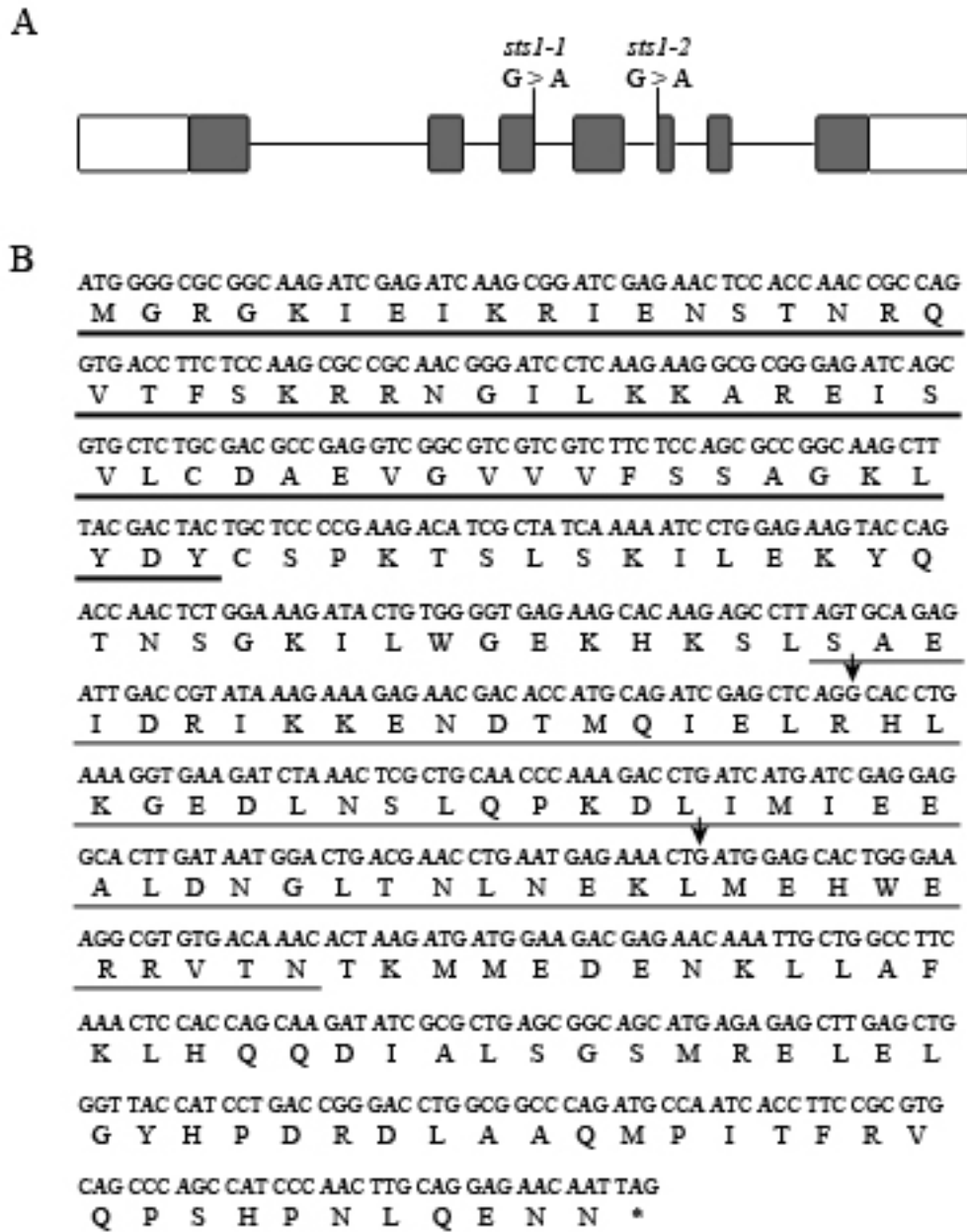GTG ACC TTC TCC AAG CGC CGC AAC GGG ATC CTC AAG AAG GCG CGG GAG ATC AGC
 V   T   F   S   K   R   R   N   G   I   L   K   K   A   R   E   I   S

GTG CTC TGC GAC GCC GAG GTC GGC GTC GTC GTC TTC TCC AGC GCC GGC AAG CTT
 V   L   C   D   A   E   V   G   V   V   V   F   S   S   A   G   K   L

TAC GAC TAC TGC TCC CCG AAG ACA TCG CTA TCA AAA ATC CTG GAG AAG TAC CAG
 Y   D   Y   C   S   P   K   T   S   L   S   K   I   L   E   K   Y   Q

ACC AAC TCT GGA AAG ATA CTG TGG GGT GAG AAG CAC AAG AGC CTT AGT GCA GAG
 T   N   S   G   K   I   L   W   G   E   K   H   K   S   L   S   A   E

ATT GAC CGT ATA AAG AAA GAG AAC GAC ACC ATG CAG ATC GAG CTC AGG CAC CTG
 I   D   R   I   K   K   E   N   D   T   M   Q   I   E   L   R   H   L

AAA GGT GAA GAT CTA AAC TCG CTG CAA CCC AAA GAC CTG ATC ATG ATC GAG GAG
 K   G   E   D   L   N   S   L   Q   P   K   D   L   I   M   I   E   E

GCA CTT GAT AAT GGA CTG ACG AAC CTG AAT GAG AAA CTG ATG GAG CAC TGG GAA
 A   L   D   N   G   L   T   N   L   N   E   K   L   M   E   H   W   E

AGG CGT GTG ACA AAC ACT AAG ATG ATG GAA GAC GAG AAC AAA TTG CTG GCC TTC
 R   R   V   T   N   T   K   M   M   E   D   E   N   K   L   L   A   F

AAA CTC CAC CAG CAA GAT ATC GCG CTG AGC GGC AGC ATG AGA GAG CTT GAG CTG
 K   L   H   Q   Q   D   I   A   L   S   G   S   M   R   E   L   E   L

GGT TAC CAT CCT GAC CGG GAC CTG GCG GCC CAG ATG CCA ATC ACC TTC CGC GTG
 G   Y   H   P   D   R   D   L   A   A   Q   M   P   I   T   F   R   V

CAG CCC AGC CAT CCC AAC TTG CAG GAG AAC AAT TAG
 Q   P   S   H   P   N   L   Q   E   N   N   *

**Figure 5.** Genomic structure of *Sts1* with lesions from the mutant alleles indicated. **(A)** A graphic representation of *Sts1* with boxes representing exons and connecting lines representing introns. The white boxes on the left and right ends of this graphic represent the 5' and 3' UTRs respectively. Positions of the EMS-induced G to A transitions in *sts1-1* and *sts1-2* are indicated. **(B)** cDNA and Protein sequence from the coding region of wild-type *Sts1*. The MADS-box (thick line) and the K domain (thin line) are underlined. Arrows indicate the bases that are replaced by As in *sts1-1* and *sts1-2*.
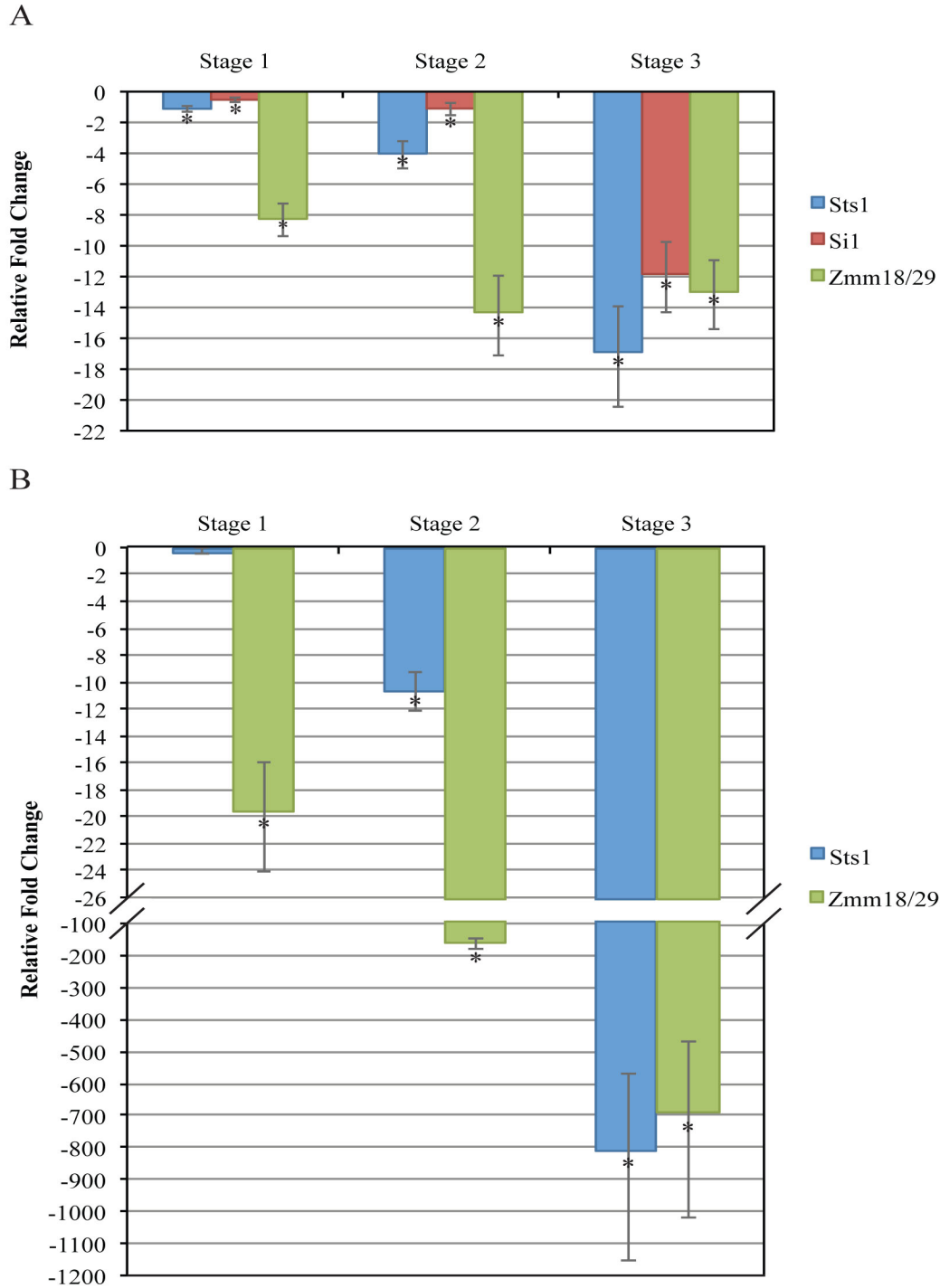
A



B



**Figure 6.** Expression of B-class genes in *sts1-1* and *si1-mum2* mutants relative to wild-type. Bars represent 2^(mean ΔΔCt for three biological replicates) and error bars represent 2^(mean ΔΔCt + SD) and 2^(mean ΔΔCt – SD). Mean fold change values that are significant at P<0.05 are marked with asterisks. **(A)** Expression of *Sts1*, *Si1*, and *Zmm18/29* in *sts1-1* male inflorescences relative to wild-type. The developmental stage of the inflorescences used in this study are indicated (i.e. Stage 1, Stage 2, and Stage 3). **(B)** Expression of *Sts1*, and *Zmm18/29* in *si1-mum2* male inflorescences relative to wild-type. The developmental stage of the inflorescences used in this study are indicated (i.e. Stage 1, Stage 2, and Stage 3).
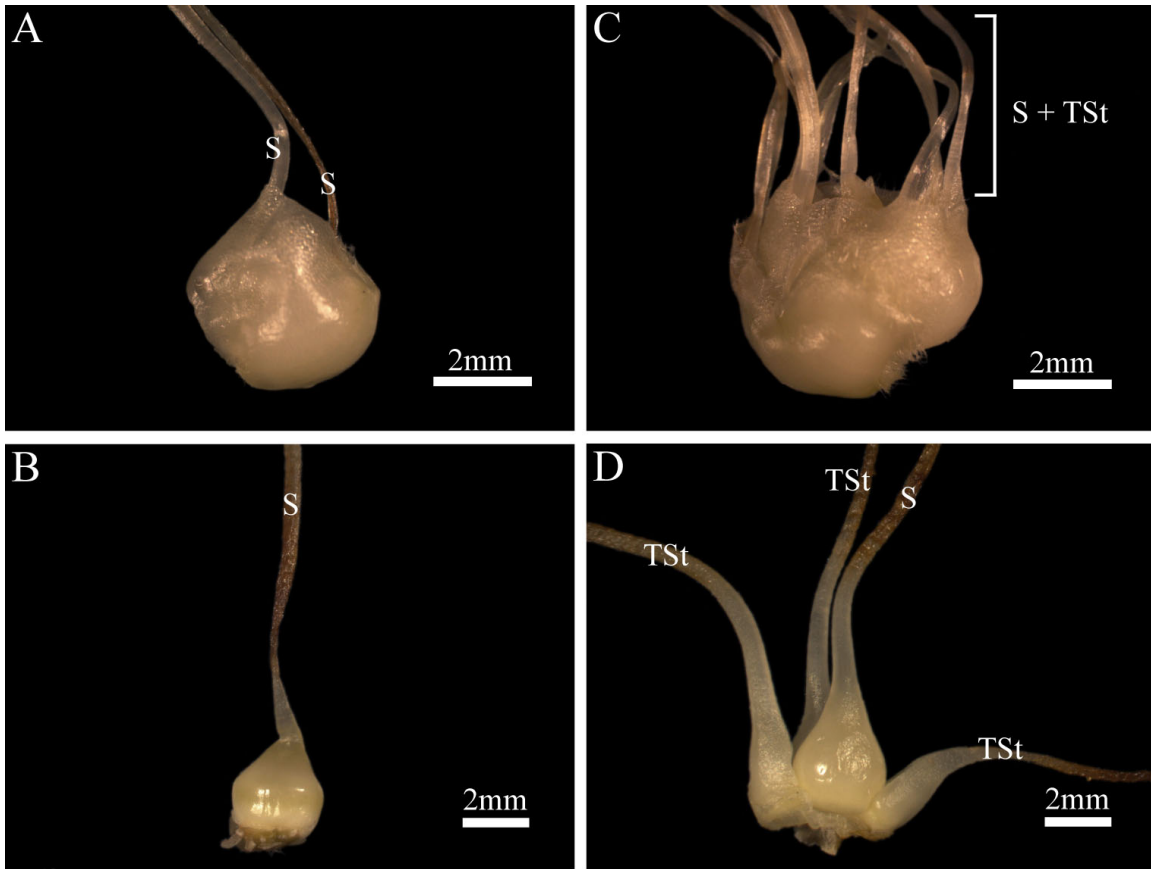
**Figure 7.** Tassel florets of *ts1* single and *ts1 sts1-1* double mutants.  **(A)** A feminized *ts1* tassel spikelet with feminized  glumes covering two florets.  Each floret has a non-aborted central gynoecium with an associated silk (S).  **(B)** A floret from (A) with glumes, lemma, and palea removed.  The floret is composed mostly of a single large gynoecium and its associated silk (S).  **(C)** A *ts1 sts1-1* tassel spikelet showing feminized glumes and silks associated with central gynoecia (S) and transformed stamens (TSt).  **(D)** A floret from (C) with glumes, lemma, and palea removed.  This floret's central gynoecium and its associated silk (S) are surrounded by three additional silks.  Each of these additional silks is associated with a carpelloid transformed stamen (TSt).
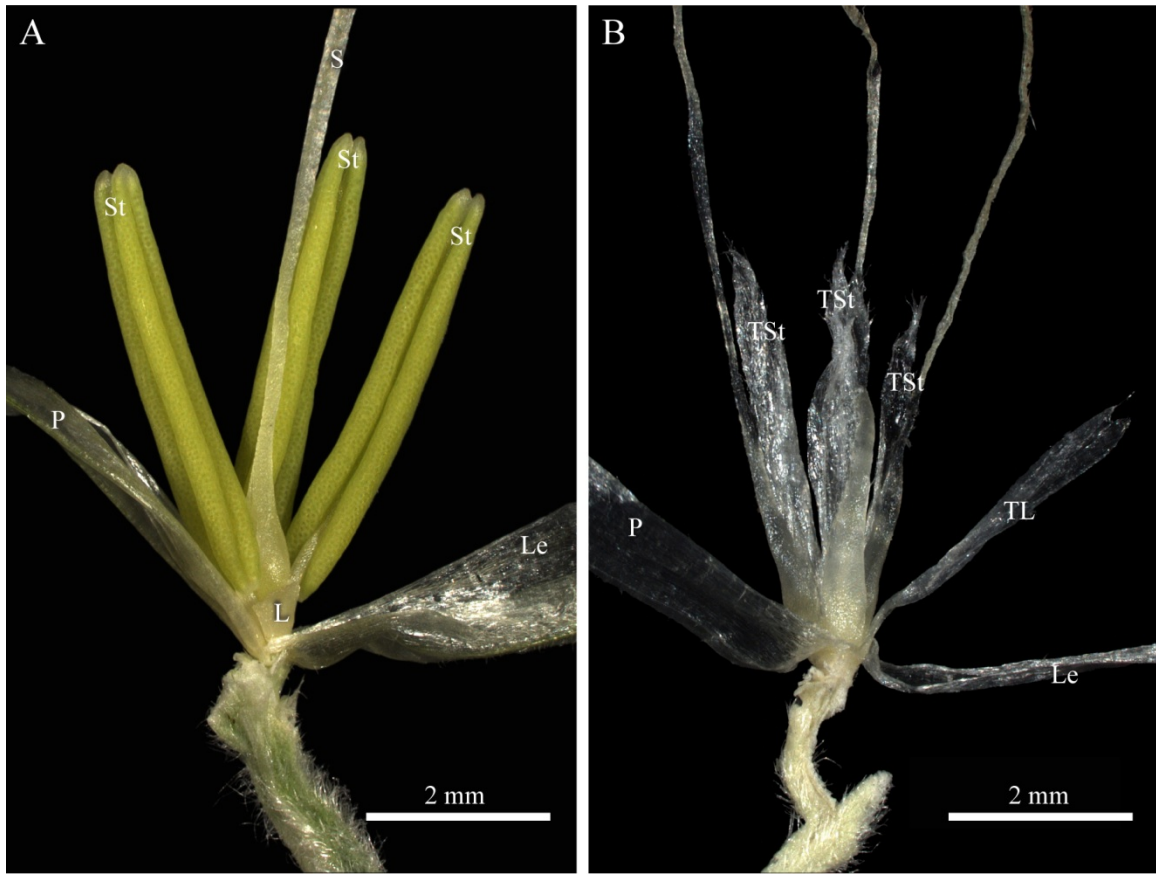
**Figure 8.** Tassel florets of *gt1-1* single and *gt1-1 sts1-1* double mutants. **(A)** A mature *gt1-1* mutant tassel floret. This floret is phenotypically similar to wild-type florets in that it has a normal lemma (Le), a normal palea (P), two normal lodicules (L), and three normal stamens (St). The *gt1* mutant floret shown here does, however, differ from wild type in that carpel growth is derepressed (i.e it has a medial carpel with an associated silk (S)). **(B)** A mature tassel floret from a *gt1-1 sts1-1* double mutant. This floret has a normal lemma (Le) and palea (P). It also has a transformed lodicule (TL) with a lemma/palea-like morphology and three transformed stamens (TSt) each with carpelloid tissue at their base and apical silks.
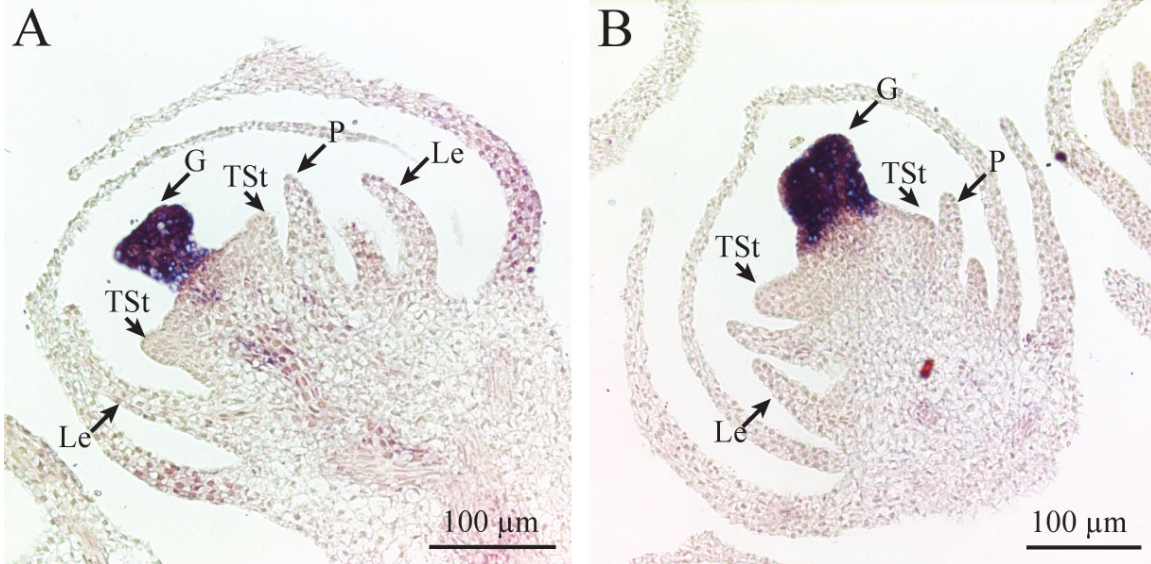
**Figure 9.** *In situ* RNA hybridization of *Gt1* in *sts1-1* tassel florets. **(A)** Longitudnal section of a *sts1-1* tassel floret showing strong expression of *Gt1* in the central gynoecium (G). *Gt1* transcriptional expression is absent in transformed stamens (TSt), lemmas (Le), and the palea (P). **(B)** Transverse section of a *sts1-1* tassel floret showing strong expression of *Gt1* in the central gynoecium (G). As in (A) *Gt1* expression is absent in transformed stamens (TSt), lemmas (Le), and the palea (P).

# REFERENCES

Acosta, I.F., Laparra, H., Romero, S.P., Schmelz, E., Hamberg, M., Mottinger, J.P., Moreno, M.A., and Dellaporta, S.L. (2009). tasselseed1 Is a Lipoxygenase Affecting Jasmonic Acid Signaling in Sex Determination of Maize. Science *323*, 262-265.

Ambrose, B.A., Lerner, D.R., Ciceri, P., Padilla, C.M., Yanofsky, M.F., and Schmidt, R.J. (2000). Molecular and genetic analyses of the silky1 gene reveal conservation in floral organ specification between eudicots and monocots. Mol Cell *5*, 569-579.

Bell, C.D., Soltis, D.E., and Soltis, P.S. (2010). The Age and Diversification of the Angiosperms Re-Revisited. Am J Bot *97*, 1296-1303.

Bensen, R.J., Johal, G.S., Crane, V.C., Tossberg, J.T., Schnable, P.S., Meeley, R.B., and Briggs, S.P. (1995). Cloning and Characterization of the Maize An1 Gene. Plant Cell *7*, 75-84.

Bowman, J.L., Smyth, D.R., and Meyerowitz, E.M. (1991). Genetic Interactions among Floral Homeotic Genes of Arabidopsis. Development *112*, 1-20.

Bradley, D., Carpenter, R., Sommer, H., Hartley, N., and Coen, E. (1993). Complementary Floral Homeotic Phenotypes Result from Opposite Orientations of a Transposon at the Plena-Locus of Antirrhinum. Cell *72*, 85-95.

Broholm, S.K., Pollanen, E., Ruokolainen, S., Tahtiharju, S., Kotilainen, M., Albert, V.A., Elomaa, P., and Teeri, T.H. (2010). Functional characterization of B class MADS-box transcription factors in Gerbera hybrida. J Exp Bot *61*, 75-85.

Cassani, E., Bertolini, E., Cerino Badone, F., Landoni, M., Gavina, D., Sirizzotti, A., and Pilu, R. (2009). Characterization of the first dominant dwarf maize mutant carrying a single amino acid insertion in the VHYNP domain of the dwarf8 gene. Mol Breeding *24*, 375-385.

Chaw, S.M., Chang, C.C., Chen, H.L., and Li, W.H. (2004). Dating the monocot-dicot divergence and the origin of core eudicots using whole chloroplast genomes. J Mol Evol *58*, 424-441.

Cheng, P.C., Greyson, R.I., and Walden, D.B. (1983). Organ Initiation and the Development of Unisexual Flowers in the Tassel and Ear of Zea-Mays. Am J Bot *70*, 450-462.

Chung, Y.Y., Kim, S.R., Kang, H.G., Noh, Y.S., Park, M.C., Finkel, D., and An, G. (1995). Characterization of two rice MADS box genes homologous to *GLOBOSA*. Plant Science *109*, 45-56.

Coen, E.S., and Meyerowitz, E.M. (1991). The War of the Whorls - Genetic Interactions Controlling Flower Development. Nature *353*, 31-37.

Davies, B., Motte, P., Keck, E., Saedler, H., Sommer, H., and Schwarz-Sommer, Z. (1999). PLENA and FARINELLI: redundancy and regulatory interactions between two Antirrhinum MADS-box factors controlling flower development. Embo J *18*, 4023-4034.

Dellaporta, S.L., and Calderonurrea, A. (1994). The Sex Determination Process in Maize. Science *266*, 1501-1505.

Ditta, G., Pinyopich, A., Robles, P., Pelaz, S., and Yanofsky, M.F. (2004). The SEP4 gene of Arabidopsis thaliana functions in floral organ and meristem identity. Curr Biol *14*, 1935-1940.

Egea-Cortines, M., Saedler, H., and Sommer, H. (1999). Ternary complex formation between the MADS-box proteins SQUAMOSA, DEFICIENS and GLOBOSA is involved in the control of floral architecture in Antirrhinum majus. Embo J *18*, 5370-5379.

Emerson, R.A., Beadle, G.W., and Fraser, A.C. (1935). A summary of linkage studies in maize. Cornell Univ Agric Exp Stn Memoir *180*, 1-83.

Frame, B.R., Shou, H.X., Chikwamba, R.K., Zhang, Z.Y., Xiang, C.B., Fonger, T.M., Pegg, S.E.K., Li, B.C., Nettleton, D.S., Pei, D.Q.*, et al.* (2002). Agrobacterium tumefaciens-mediated transformation of maize embryos using a standard binary vector system. Plant Physiol *129*, 13-22.

Geuten, K., and Irish, V. (2010). Hidden Variability of Floral Homeotic B Genes in Solanaceae Provides a Molecular Basis for the Evolution of Novel Functions. Plant Cell *22*, 2562-2578.

Goto, K., and Meyerowitz, E.M. (1994). Function and Regulation of the Arabidopsis Floral Homeotic Gene Pistillata. Gene Dev *8*, 1548-1560.

Hama, E., Takumi, S., Ogihara, Y., and Murai, K. (2004). Pistillody is caused by alterations to the class-B MADS-box gene expression pattern in alloplasmic wheats. Planta *218*, 712-720.

Hedden, P., and Phinney, B.O. (1979). Comparison of Ent-Kaurene and Ent-Isokaurene Synthesis in Cell-Free Systems from Etiolated Shoots of Normal and Dwarf-5 Maize Seedlings. Phytochemistry *18*, 1475-1479.

Hill, T.A., Day, C.D., Zondlo, S.C., Thackeray, A.G., and Irish, V.F. (1998). Discrete spatial and temporal cis-acting elements regulate transcription of the Arabidopsis floral homeotic gene APETALA3. Development *125*, 1711-1721.

Honma, T., and Goto, K. (2001). Complexes of MADS-box proteins are sufficient to convert leaves into floral organs. Nature *409*, 525-529.

Huang, H., Mizukami, Y., Hu, Y., and Ma, H. (1993). Isolation and Characterization of the Binding Sequences for the Product of the Arabidopsis Floral Homeotic Gene Agamous. Nucleic Acids Res *21*, 4769-4776.

Huijser, P., Klein, J., Lonnig, W.E., Meijer, H., Saedler, H., and Sommer, H. (1992). Bracteomania, an Inflorescence Anomaly, Is Caused by the Loss of Function of the Mads-Box Gene Squamosa in Antirrhinum-Majus. Embo J *11*, 1239-1249.

Immink, R.G.H., Gadella, T.W.J., Ferrario, S., Busscher, M., and Angenent, G.C. (2002). Analysis of MADS box protein-protein interactions in living plant cells. P Natl Acad Sci USA *99*, 2416-2421.

Immink, R.G.H., Kaufmann, K., and Angenent, G.C. (2010). The 'ABC' of MADS domain protein behaviour and interactions. Semin Cell Dev Biol *21*, 87-93.

Irish, E.E. (1996). Regulation of sex determination in maize. Bioessays *18*, 363-369.

Jack, T., Brockman, L.L., and Meyerowitz, E.M. (1992). The Homeotic Gene Apetala3 of Arabidopsis-Thaliana Encodes a Mads Box and Is Expressed in Petals and Stamens. Cell *68*, 683-697.

Jackson, D., Veit, B., and Hake, S. (1994). Expression of Maize Knotted1 Related Homeobox Genes in the Shoot Apical Meristem Predicts Patterns of Morphogenesis in the Vegetative Shoot. Development *120*, 405-413.

Jofuku, K.D., Denboer, B.G.W., Vanmontagu, M., and Okamuro, J.K. (1994). Control of Arabidopsis Flower and Seed Development by the Homeotic Gene Apetala2. Plant Cell *6*, 1211-1225.

Joppa, L.N., Roberts, D.L., and Pimm, S.L. (2011). How many species of flowering plants are there? P Roy Soc B-Biol Sci *278*, 554-559.

Kater, M.M., Franken, J., Carney, K.J., Colombo, L., and Angenent, G.C. (2001). Sex determination in the monoecious species cucumber is confined to specific floral whorls. Plant Cell *13*, 481-493.

Keck, E., McSteen, P., Carpenter, R., and Coen, E. (2003). Separation of genetic functions controlling organ identity in flowers. Embo J *22*, 1058-1066.

Kim, S.T., Yoo, M.J., Albert, V.A., Farris, J.S., Soltis, P.S., and Soltis, D.E. (2004). Phylogeny and diversification of B-function MADS-box genes in angiosperms: Evolutionary and functional implications of a 260-million-year-old duplication. Am J Bot *91*, 2102-2118.

Kramer, E.M., Dorit, R.L., and Irish, V.F. (1998). Molecular evolution of genes controlling petal and stamen development: Duplication and divergence within the APETALA3 and PISTILLATA MADS-box gene lineages. Genetics *149*, 765-783.

Krizek, B.A., and Meyerowitz, E.M. (1996a). The Arabidopsis homeotic genes APETALA3 and PISTILLATA are sufficient to provide the B class organ identity function. Development *122*, 11-22.

Krizek, B.A., and Meyerowitz, E.M. (1996b). Mapping the protein regions responsible for the functional specificities of the *Arabidopsis* MADS domain organ-identity proteins. P Natl Acad Sci USA *93*, 4063-4070.

Li, J., Jiang, D., Zhou, H., Li, F., Yang, J., Hong, L., Fu, X., Li, Z., Liu, Z., and Zhuang, C. (2011). Expression of RNA-interference/antisense transgenes by the cognate promoters of target genes is a better gene-silencing strategy to study gene functions in rice. PLoS One *6*, e17444.

Liljegren, S.J., Ditta, G.S., Eshed, H.Y., Savidge, B., Bowman, J.L., and Yanofsky, M.F. (2000). Shatterproof Mads-Box Genes Control Seed Dispersal in Arabidopsis. Nature *404*, 766-770.

Livak, K.J., and Schmittgen, T.D. (2001). Analysis of relative gene expression data using real-time quantitative PCR and the 2(T)(-Delta Delta C) method. Methods *25*, 402-408.

Magallon, S. (2010). Using Fossils to Break Long Branches in Molecular Dating: A Comparison of Relaxed Clocks Applied to the Origin of Angiosperms. Syst Biol *59*, 384-399.

Mandel, M.A., Gustafsonbrown, C., Savidge, B., and Yanofsky, M.F. (1992). Molecular Characterization of the Arabidopsis Floral Homeotic Gene Apetala1. Nature *360*, 273-277.

McGonigle, B., Bouhidel, K., and Irish, V. (1996). Nuclear localization of the Arabidopsis APETALA3 and PISTILLATA homeotic gene products depends on their simultaneous expression (vol 10, pg 1812, 1996). Gene Dev *10*, 2235-2235.

Michelmore, R.W., Paran, I., and Kesseli, R.V. (1991). Identification of Markers Linked to Disease-Resistance Genes by Bulked Segregant Analysis - a Rapid Method to Detect Markers in Specific Genomic Regions by Using Segregating Populations. P Natl Acad Sci USA *88*, 9828-9832.

Mitchell, C.H., and Diggle, P.K. (2005). The evolution of unisexual flowers: morphological and functional convergence results from diverse developmental transitions. Am J Bot *92*, 1068-1076.

Mizukami, Y., and Ma, H. (1992). Ectopic Expression of the Floral Homeotic Gene Agamous in Transgenic Arabidopsis Plants Alters Floral Organ Identity. Cell *71*, 119-131.

Moon, Y.H., Jung, J.Y., Kang, H.G., and An, G.H. (1999). Identification of a rice APETALA3 homologue by yeast two-hybrid screening. Plant Mol Biol *40*, 167-177.

Munster, T., Wingen, L.U., Faigl, W., Werth, S., Saedler, H., and Theissen, G. (2001). Characterization of three GLOBOSA-like MADS-box genes from maize: evidence for ancient paralogy in one class of floral homeotic B-function genes of grasses. Gene *262*, 1-13.

Nagasawa, N., Miyoshi, M., Sano, Y., Satoh, H., Hirano, H., Sakai, H., and Nagato, Y. (2003). SUPERWOMAN1 and DROOPING LEAF genes control floral organ identity in rice. Development *130*, 705-718.

Neuffer, G.M. (1994). Mutagenesis. In The Maize Handbook, M. Freeling, ed. (New York, Springer-Verlag), pp. 212-218.

Nickerson, N.H., and Dale, E.E. (1955). Tassel modification in *Zea mays*. Ann Mo Bot Gard *42*, 195-211.

Okamuro, J.K., Caster, B., Villarroel, R., VanMontagu, M., and Jofuku, K.D. (1997). The AP2 domain of APETALA2 defines a large new family of DNA binding proteins in Arabidopsis. P Natl Acad Sci USA *94*, 7076-7081.

Park, J.H., Ishikawa, Y., Ochiai, T., Kanno, A., and Kameya, T. (2004). Two GLOBOSA-like genes are expressed in second and third whorls of homochlamydeous flowers in Asparagus officinalis L. Plant Cell Physiol *45*, 325-332.

Park, J.H., Ishikawa, Y., Yoshida, R., Kanno, A., and Kameya, T. (2003). Expression of AODEF, a B-functional MADS-box gene, in stamens and inner tepals of the dioecious species Asparagus officinalis L. Plant Mol Biol *51*, 867-875.

Paterson, A.H., Bowers, J.E., and Chapman, B.A. (2004). Ancient polyploidization predating divergence of the cereals, and its consequences for comparative genomics. P Natl Acad Sci USA *101*, 9903-9908.

Paz, M.M., Shou, H.X., Guo, Z.B., Zhang, Z.Y., Banerjee, A.K., and Wang, K. (2004). Assessment of conditions affecting Agrobacterium-mediated soybean transformation using the cotyledonary node explant. Euphytica *136*, 167-179.

Pelaz, S., Ditta, G.S., Baumann, E., Wisman, E., and Yanofsky, M.F. (2000). B and C floral organ identity functions require SEPALLATA MADS-box genes. Nature *405*, 200-203.

Phinney, B.O., and Spray, C.R. (1982). Chemical genetics and the gibberellin pathway in *Zea mays L.* In Plant Growth Substances, P.F. Wareing, ed. (New York, Academic Press), pp. 101-110.

Phipps, I.F. (1928). Heritable characters in maize: XXXI *Tassel-seed* 4. J hered *19*, 399-404.

Riechmann, J.L., Krizek, B.A., and Meyerowitz, E.M. (1996). Dimerization specificity of Arabidopsis MADS domain homeotic proteins APETALA1, APETALA3, PISTILLATA, and AGAMOUS. P Natl Acad Sci USA *93*, 4793-4798.

Schwarz-Sommer, Z., Hue, I., Huijser, P., Flor, P.J., Hansen, R., Tetens, F., Lonnig, W.E., Saedler, H., and Sommer, H. (1992). Characterization of the Antirrhinum Floral Homeotic Mads-Box Gene Deficiens - Evidence for DNA-Binding and Autoregulation of Its Persistent Expression Throughout Flower Development. Embo J *11*, 251-263.

Senthil-Kumar, M., and Mysore, K.S. (2011). Caveat of RNAi in plants: the off-target effect. Methods Mol Biol *744*, 13-25.

Smith, S.A., Beaulieu, J.M., and Donoghue, M.J. (2010). An uncorrelated relaxed-clock analysis suggests an earlier origin for flowering plants. P Natl Acad Sci USA *107*, 5897-5902.

Sommer, H., Beltran, J.P., Huijser, P., Pape, H., Lonnig, W.E., Saedler, H., and Schwarzsommer, Z. (1990). Deficiens, a Homeotic Gene Involved in the Control of Flower Morphogenesis in Antirrhinum-Majus - the Protein Shows Homology to Transcription Factors. Embo J *9*, 605-613.

Song, J.J., Ma, W., Tang, Y.J., Chen, Z.Y., and Liao, J.P. (2010). Isolation and Characterization of Three MADS-box Genes from Alpinia hainanensis (Zingiberaceae). Plant Mol Biol Rep *28*, 264-276.

Spray, C.R., Kobayashi, M., Suzuki, Y., Phinney, B.O., Gaskin, P., and MacMillan, J. (1996). The dwarf-1 (d1) mutant of Zea mays blocks three steps in the gibberellin-biosynthetic pathway. P Natl Acad Sci USA *93*, 10515-10518.

Theissen, G., and Saedler, H. (2001). Plant biology - Floral quartets. Nature *409*, 469-471.

Trobner, W., Ramirez, L., Motte, P., Hue, I., Huijser, P., Lonnig, W.E., Saedler, H., Sommer, H., and Schwarzsommer, Z. (1992). Globosa - a Homeotic Gene Which Interacts with Deficiens in the Control of Antirrhinum Floral Organogenesis. Embo J *11*, 4693-4704.

Urbanus, S.L., de Folter, S., Shchennikova, A.V., Kaufmann, K., Immink, R.G.H., and Angenent, G.C. (2009). In planta localisation patterns of MADS domain proteins during floral development in Arabidopsis thaliana. Bmc Plant Biol *9*.

Vandenbussche, M., Zethof, J., Royaert, S., Weterings, K., and Gerats, T. (2004). The duplicated B-class heterodimer model: Whorl-specific effects and complex genetic interactions in Petunia hybrida flower development. Plant Cell *16*, 741-754.

Vicentini, A., Barber, J.C., Aliscioni, S.S., Giussani, L.M., and Kellogg, E.A. (2008). The age of the grasses and clusters of origins of C(4) photosynthesis. Global Change Biol *14*, 2963-2977.

West, A.G., Causier, B.E., Davies, B., and Sharrocks, A.D. (1998). DNA binding and dimerisation determinants of Antirrhinum majus MADS-box transcription factors. Nucleic Acids Res *26*, 5277-5287.

Whipple, C.J., Ciceri, P., Padilla, C.M., Ambrose, B.A., Bandong, S.L., and Schmidt, R.J. (2004). Conservation of B-class floral homeotic gene function between maize and Arabidopsis. Development *131*, 6083-6091.

Whipple, C.J., Kebrom, T.H., Weber, A.L., Yang, F., Hall, D., Meeley, R., Schmidt, R., Doebley, J., Brutnell, T.P., and Jackson, D.P. (2011). grassy tillers1 promotes apical dominance in maize and responds to shade signals in the grasses. P Natl Acad Sci USA *108*, E506-E512.

Whipple, C.J., Zanis, M.J., Kellogg, E.A., and Schmidt, R.J. (2007). Conservation of B class gene expression in the second whorl of a basal grass and outgroups links the origin of lodicules and petals. P Natl Acad Sci USA *104*, 1081-1086.

Winkler, R.G., and Freeling, M. (1994). Physiological Genetics of the Dominant Gibberellin-Nonresponsive Maize Dwarfs, Dwarf-8 and Dwarf-9. Planta *193*, 341-348.

Winkler, R.G., and Helentjaris, T. (1995). The Maize Dwarf3 Gene Encodes a Cytochrome P450-Mediated Early Step in Gibberellin Biosynthesis. Plant Cell *7*, 1307-1317.

Yampolsky, C., and Yampolsky, H. (1922). Distribution of sex forms in the phanerogamic flora. Bibliotheca Genet *3*, 1-59.

Yanofsky, M.F., Ma, H., Bowman, J.L., Drews, G.N., Feldmann, K.A., and Meyerowitz, E.M. (1990). The Protein Encoded by the Arabidopsis Homeotic Gene Agamous Resembles Transcription Factors. Nature *346*, 35-39.

Yao, S.G., Ohmori, S., Kimizu, M., and Yoshida, H. (2008). Unequal genetic redundancy of rice PISTILLATA orthologs, OsMADS2 and OsMADS4, in lodicule and stamen development. Plant Cell Physiol *49*, 853-857.